

Antonio Luna
Joan C. Vilanova
L. Celso Hygino da Cruz Jr.
Santiago E. Rossi *Editors*

Functional Imaging in Oncology

Clinical Applications

Volume 2

 Springer

Functional Imaging in Oncology

Antonio Luna • Joan C. Vilanova
L. Celso Hygino da Cruz Jr.
Santiago E. Rossi
Editors

Functional Imaging in Oncology

Clinical Applications - Volume 2

 Springer

Editors

Antonio Luna
Chief of MRI
Health Time Group
Jaén
Spain

L. Celso Hygino da Cruz Jr.
Department of Radiology
CDPI and IRM
Rio de Janeiro, RJ
Brazil

Department of Radiology
University Hospitals
Case Western Reserve University
Cleveland, Ohio
USA

Santiago E. Rossi
Centro de Diagnóstico
Dr. Enrique Rossi
Buenos Aires
Argentina

Joan C. Vilanova
Chief of MRI
Clínica Girona - Hospital Sta. Caterina
Ass. Professor. University of Girona
Girona
Spain

ISBN 978-3-642-40581-5 ISBN 978-3-642-40582-2 (eBook)
DOI 10.1007/978-3-642-40582-2
Springer Heidelberg New York Dordrecht London

Library of Congress Control Number: 2013956347

© Springer-Verlag Berlin Heidelberg 2014

This work is subject to copyright. All rights are reserved by the Publisher, whether the whole or part of the material is concerned, specifically the rights of translation, reprinting, reuse of illustrations, recitation, broadcasting, reproduction on microfilms or in any other physical way, and transmission or information storage and retrieval, electronic adaptation, computer software, or by similar or dissimilar methodology now known or hereafter developed. Exempted from this legal reservation are brief excerpts in connection with reviews or scholarly analysis or material supplied specifically for the purpose of being entered and executed on a computer system, for exclusive use by the purchaser of the work. Duplication of this publication or parts thereof is permitted only under the provisions of the Copyright Law of the Publisher's location, in its current version, and permission for use must always be obtained from Springer. Permissions for use may be obtained through RightsLink at the Copyright Clearance Center. Violations are liable to prosecution under the respective Copyright Law.

The use of general descriptive names, registered names, trademarks, service marks, etc. in this publication does not imply, even in the absence of a specific statement, that such names are exempt from the relevant protective laws and regulations and therefore free for general use.

While the advice and information in this book are believed to be true and accurate at the date of publication, neither the authors nor the editors nor the publisher can accept any legal responsibility for any errors or omissions that may be made. The publisher makes no warranty, express or implied, with respect to the material contained herein.

Printed on acid-free paper

Springer is part of Springer Science+Business Media (www.springer.com)

*To my parents for forming me into what I am today
With all my love to my Marias for their patience and support*
Antonio

*To my wife Cris for her patience and understanding; and to our
daughter Cristina, and son Eduard, with love*
Kai

*To my parents, Luiz Celso and Leonice, as well as to my wife
Simone, for their support and understanding during the process
of preparing this work*
Celso

*To my friend and mentor Jeremy Erasmus
To my family and my wife Clara*
Santiago

Foreword

Molecular and functional imaging can improve the diagnosis, treatment and outcomes in oncologic patients. The ability to non-invasively visualize, characterize and quantify biologic processes at the cellular, molecular and genetic level presents a new era in oncology. This book provides a practical approach to the different imaging techniques used to obtain and understand this functional information. The editors, Drs. Luna, Vilanova, Da Cruz and Rossi are well-renowned radiologists experienced in functional and molecular imaging. They have assembled an international group of acclaimed experts that complement their expertise and have written a two volume tour de force on state-of-the-art functional imaging useful in the assessment and management of oncologic patients. This comprehensive review was a pleasure to read and will undoubtedly become an indispensable resource for clinicians-in-training as well as practicing radiologists and oncologists. The authors are adept at simplifying complexity and their ambitious effort provides a complete review of diffusion MRI, perfusion CT and MRI, dual-energy CT, spectroscopy, dynamic contrast-enhanced ultrasonography, and positron emission tomography (PET). The text is clearly written and complemented by numerous high-quality illustrations that highlight key features and major teaching points. The first volume explains the biologic basis of the functional imaging modalities and provides meaningful clinical insight and understanding of the techniques used in the imaging of angiogenesis, tumor metabolism and hypoxia. The second volume considers specific malignancies and the use and benefit of the different imaging modalities in the diagnosis, prediction of treatment outcome, and early evaluation of treatment response in oncologic patients. The chapters are concise and comprehensive enough for the reader to obtain a firm foundation in the essential aspects of the topic reviewed. In fact, both volumes 1 and 2 impart knowledge in an easy to read, concise, coherent format. It is impossible to over-applaud the clarity and well-written and structured format of these books. In summary, the authors have used their experience to write an excellent textbook and the scope, structure and attention to detail are superb. The topics are well focused and this wide-ranging review is an invaluable guide to functional imaging. This is a thoughtful and well-developed book that is without doubt an excellent, comprehensive text of the essentials required to understand and use functional imaging.

Houston, TX, USA

Jeremy J. Erasmus

Preface

In the last decades, comprehensive cancer care and research have been both critically dependent on imaging. The role of anatomical imaging with ultrasound, CT and MRI has grown progressively. Application of medical imaging in cancer patients has expanded from diagnosis and staging to screening, guide for treatment, therapeutic monitoring, detection of recurrence and prediction of treatment response. The role of imaging has changed due in part to the introduction of functional imaging with PET at the end of the last century.

Recent advances in cellular biology, molecular biology and genetics have led to a better understanding of biological bases of cancer. These advances in oncology biologics and development of new biological therapies and treatment options have produced a paradigm shift in cancer treatment. In many clinical scenarios, cancer is now considered a chronic disease instead of an untreatable malignancy. Furthermore, the approach to cancer management is moving from treating diseases to personalized therapies. All these major changes need multidisciplinary teams where experts in biomedical imaging are and will be an important part of the puzzle. Very wide scales have to be covered by imaging, from the molecular and cellular level to organ to whole organism for clinical staging. Combined functional and anatomical imaging techniques are necessary to visualize and target different aspects of cancer. At this point, functional and molecular imaging might transform and improve all phases of cancer management.

Functional imaging using biomarkers can assess and quantify biological characteristics of tumors by a wide range of techniques. Ultrasound can explore tumor angiogenesis and tissue elasticity by means of contrast-enhanced acquisitions and elastography, respectively. New CT approaches such as CT-perfusion and spectral energy CT have broadened the knowledge of tumor angiogenesis and tissue characteristics. Furthermore, MRI is now able to develop multiparametric studies of a tumor in a single study, being possible to analyze tumor cellularity, angiogenesis, hypoxia and metabolism simultaneously using diffusion-weighted, dynamic contrast-enhanced, BOLD and spectroscopic sequences, respectively. PET and multimodality (hybrid) imaging have also expanded their applications with the use of other metabolites different to 18-FDG. Therefore, it is possible to explore different cancer hallmarks, such as angiogenesis, metabolism or hypoxia. The development of new approaches such as optical imaging, nanocomposites, novel imaging probes for PET and MRI permit to target different molecular and cellular processes. All these developments are directed to cancer phenotyping

by imaging techniques. The advances in functional and molecular imaging have laid to apply imaging as a cancer biomarker; to help direct cancer treatment in a way that is complementary to plans based on tissue- and blood-based biomarkers. The ability to measure in vivo cancer biology with functional imaging during treatment provides a unique opportunity to identify and select the therapy that's most likely to successfully treat an individual patient's cancer. In a near future, new methodologies will deal with theranostics, looking for a combined and simultaneous diagnosis and treatment of the disease.

The purpose of this book is to provide a useful manual to be used by the wide range and variety of disciplines involved in the management of oncologic patients, including radiologists, nuclear medicine specialists and oncologists. We have tried to cover and provide all the extensive information related to the different imaging modalities in clinical use and research from the technical bases to clinical applications. The book is divided in two volumes and 13 parts. The first volume is focused on the biophysical basis and technical approaches of functional imaging techniques. This first volume is divided in four parts. The first part covers a general approach to cancer biology, imaging biomarkers and role of functional and molecular imaging in diagnosis and treatment. The three following parts deal with the role of functional and molecular imaging in the study of cancer hallmarks and review their technical basis and applications in clinical practice and research. This part of the book is organized by different imaging techniques in separate chapters to stress the importance of an adequate imaging technique and acquisition to optimize the performance of each technique. The second volume of the book is the largest, where the main types of cancers are addressed in different chapters and organized by organ systems. In each of these chapters, the role of functional imaging in the management of different tumor types is discussed.

This book has been possible due to the generous effort of all contributing authors. All of them, well-known experts in their respective fields, have shared with us their experience in cutting-edge topics. It has been a pleasure to coordinate such a great team, making editing of this book a learning and enjoyable process.

Finally, we would like to acknowledge the enormous support of Dr. Jeremy J. Erasmus in the first conception of this book and Dr. Roberto Garcia-Figueiras for his help in the organization of the contents.

We hope that this book can be helpful for all interested in cancer imaging, and readers may share some of the learning and enjoyment we had editing this book.

Jaén, Spain
Girona, Spain
Rio de Janeiro, Brazil
Buenos Aires, Argentina

Antonio Luna
Joan C. Vilanova
L. Celso Hygino Da Cruz
Santiago E. Rossi

Contents

Volume 2 Clinical Applications

Part V Tumors of the CNS and Spinal Cord

- 24 Functional Magnetic Resonance Techniques in CNS Tumors** 553
Antônio José da Rocha, Antonio Carlos Martins Maia Jr,
and Suzana Maria Fleury Malheiros
- 25 MR Imaging Evaluation of Posttreatment Changes in Brain Neoplasms** 603
L. Celso Hygino da Cruz Jr, Raquel Ribeiro Batista,
and Claudio de Carvalho Rangel
- 26 Metastasis and Other Tumors of the CNS** 641
Adam Wilner, Eytan Raz, Edmond Knopp,
and Girish Fatterpekar
- 27 Spinal Cord Tumors: Anatomic and Advanced Imaging** 683
Mauricio Castillo and Majda M. Thurnher
- 28 Head and Neck Cancer** 703
Inmaculada Rodríguez Jiménez, María Nieves Cabrera Martín,
Antonio Luna, and José Luis Carreras Delgado

Part VI Chest Malignancies

- 29 Lung Cancer: PET, Perfusion CT, and Functional MR Imaging** 723
Santiago E. Rossi, Carmen Trinidad,
and Antonio Luna
- 30 Functional Imaging of Malignant Pleural Mesothelioma and other Pleural and Chest Wall Lesions** 751
Jordi Broncano, Maria José García-Velloso,
Teodoro Martin-Noguerol, and Antonio Luna
- 31 Thymomas and Other Thymic Primary Malignancies of the Chest** 771
Marcelo F.K. Benveniste

32	Functional Imaging in Cardiac Tumors	789
	Carlos S. Restrepo, Sina Tavakoli, and Sonia L. Betancourt	
Part VII Women's Cancers		
33	Breast Cancer	813
	Elizabeth A.M. O'Flynn	
34	PET-CT of Gynecological Malignancies and Ovarian Cancer	839
	P. Caroli and S. Fanti	
35	Functional MRI of Uterine (Endometrial and Cervical) Cancer	851
	Jennifer C. Wakefield, Kate Downey, and Nandita M. deSouza	
36	Functional Imaging of Ovarian Cancer and Peritoneal Carcinomatosis	877
	Stavroula Kyriazi, Jennifer C. Wakefield, and Nandita M. deSouza	
Part VIII Malignancies of the Gastrointestinal System		
37	Esophagus, Stomach, and Small Bowel Malignancies	903
	Cristina Rodríguez-Rey, Aída Ortega-Candil, and Ramiro Jesús Méndez Fernández	
38	Colorectal Cancer	923
	Roberto García-Figueiras, Sandra Baleato-González, Antonio Gómez-Caamaño, Ana Alvarez-Castro, and Jesús Paredes-Cotoré	
Part IX Hepatobiliary and Pancreatic Malignancies		
39	Overview of Functional Imaging Techniques for Liver Malignancies in Current Clinical Practice or in a Very Near Future	951
	Antonio Luna, Guilherme Moura Cunha, Rocío Sánchez-Sánchez, and Antonio Rodríguez-Fernández	
40	Hepatocellular Carcinoma	987
	Jordi Rimola and Carmen Ayuso	
41	Role of Functional MRI in the Management of Liver Metastases	1003
	Leonardo Kayat Bittencourt, Romulo Varella de Oliveira, and Bachir Taouli	
42	Other Malignant Lesions of the Liver	1025
	Giovanni Morana, Riccardo Zanato, and Onorina Bruno	

43	Functional Imaging of Gallbladder and Biliary Malignancies	1065
	Mariano Volpacchio and Joaquina López Moras	
44	Pancreatic Adenocarcinoma and Other Pancreatic Malignancies	1077
	Antonio Luna, Lidia Alcalá-Mata, Mariano Volpacchio, and José Pablo Martínez-Barbero	
45	Splenic Lesions	1111
	Shiva Gupta, Sandeep P. Deshmukh, Matthew G. Ditzler, and Khaled M. Elsayes	
Part X Genitourinary Tract Tumors		
46	Functional Imaging of Renal Cell Carcinoma	1143
	Carmen Sebastià, Antonio Luna, Pilar Paredes, and Carlos Nicolau	
47	Functional CT and MRI of the Urinary System and Adrenal Glands	1173
	Soichiro Yoshida, Hitoshi Masuda, Fumitaka Koga, Hiroshi Tanaka, and Kazunori Kihara	
48	Prostate Cancer	1183
	Joan C. Vilanova, Maria Boada, and Joaquim Barceló	
49	Scrotum	1207
	Sandra Baleato-González, Luis León Mateos, María Isolina Pérez Santiago, and Joan C. Vilanova	
50	Functional Imaging of Tumors of the Mesenterium and Retroperitoneum	1235
	Akira Toriihara and Ukihide Tateishi	
Part XI Malignancies of the Endocrine System		
51	Functional Oncological Imaging of the Endocrine System . . .	1249
	Ka Kit Wong, Asha Kandathil, Domenico Rubello, and Milton D. Gross	
Part XII Hematological Malignancies		
52	Functional Imaging in Clinical Use for the Assessment of Lymph Nodes in Oncological Patients	1271
	Teodoro Martín Noguerol, Rocío Sánchez Sánchez, José Pablo Martínez Barbero, Antonio Rodríguez Fernández, and Antonio Luna	
53	Functional Imaging in Lymphoma	1311
	Chieh Lin, Emmanuel Itti, Alain Luciani, Yenlin Huang, Corinne Haioun, Violaine Safar, Tzu-Chen Yen, and Alain Rahmouni	

54 Multiple Myeloma and Other Hematological Malignancies	1335
Jens Hillengass and Tobias Bäuerle	
Part XIII Malignant Tumors of the Musculoskeletal System	
55 Advanced MRI Techniques of Soft Tissue Tumors	1357
Flávia Costa, Clarissa Canella, Pedro Henrique Martins, and Silvana Mendonça	
56 Bone Malignancies	1369
J.L. Bloem, Carla van Rijswijk, and Herman M. Kroon	
57 Bone Metastasis	1389
Tobias Bäuerle	
58 Functional Imaging of Pediatric Malignancies	1411
Alexander J. Towbin and Andrew T. Trout	
59 Malignant Melanoma	1443
Aída Ortega-Candil, Cristina Rodríguez-Rey, and Jose Luis Carreras-Delgado	
Index	1457

Volume 1 Biophysical Basis and Technical Approaches**Part I Clinical and Therapeutic Approach to Functional Oncological Imaging**

- 1 Cancer Biology: What's Important for Imaging**
Jose L. Vercher Conejero, Zhenghong Lee, and Pablo R. Ros
- 2 Imaging Biomarkers and Surrogate Endpoints in Oncology Clinical Trials**
Richard G. Abramson and Thomas E. Yankeelov
- 3 Role of Molecular Imaging in the Era of Personalized Medicine: A Review**
Evis Sala, Hebert Alberto Vargas, Olivio F. Donati, Wolfgang A. Weber, and Hedvig Hricak
- 4 Radiotherapy and Imaging**
Ursula Nestle and Anca-Ligia Grosu
- 5 New Therapies and Functional-Molecular Imaging**
Roberto García Figueiras and Anwar R. Padhani
- 6 Medical Image Computing for Oncology: Review and Clinical Examples**
Zhong Xue and Stephen T.C. Wong

Part II Imaging of Cancer Hallmarks

- 7 Imaging Angiogenesis**
Alan Jackson and James P.B. O'Connor
- 8 Imaging of Tumor Metabolism: MR Spectroscopy**
Asif Rizwan and Kristine Glunde
- 9 Imaging of Tumour Metabolism: 18-FDG PET**
Michael Lin and Divesh Kumar
- 10 Imaging of Tumor Metabolism: PET with Other Metabolites**
Chi-Lai Ho, Sirong Chen, and Man-Ki Cheung
- 11 Current Clinical Imaging of Hypoxia with PET and Future Perspectives**
Mareike Roscher, Carmen Wängler, Stefan O. Schönberg, and Björn Wängler
- 12 MRI Hypoxia Measurements**
Stefanie Remmele, Ralph P. Mason, and James P.B. O'Connor

Part III Functional Imaging Techniques in Clinical Use

- 13 Overview of Functional MR, CT, and US Imaging Techniques in Clinical Use**
Ewelina Kluza, Doenja M.J. Lambregts,
and Regina G.H. Beets-Tan
- 14 Diffusion-Weighted MR Imaging**
Henry H. Tam and Dow-Mu Koh
- 15 Perfusion CT: Principles, Technical Aspects and Applications in Oncology**
Olwen Westerland and Vicky Goh
- 16 Perfusion Imaging by Magnetic Resonance**
Javier Sánchez González, Antonio Luna,
and L. Celso Hygino da Cruz, Jr.
- 17 DCE-US: Evaluation of Angiogenesis**
Nathalie Lassau
- 18 Spectroscopy of Cancer**
Natalie J. Serkova
- 19 Hybrid Imaging: PET-CT and PET-MRI**
Barbara Malene Fischer and Johan Löfgren
- 20 Dual-Energy and Spectral Energy Computed Tomography: Oncological Body Applications in Clinical Use**
Alvin C. Silva and Wendy Z. Stiles
- 21 US Elastography: Applications in Tumors**
Richard G. Barr

Part IV Molecular Imaging Techniques in Clinical Use and in Research

- 22 New Molecular and Functional Imaging Techniques**
Vanessa Gómez-Vallejo, María Jiménez-González, Jordi Llop,
and Torsten Reese
- 23 Multiparametric Imaging**
Luis Martí-Bonmatí, Ángel Alberich-Bayarri,
Gracián García-Martí, and Roberto Sanz-Requena

Index

Part V

Tumors of the CNS and Spinal Cord

Antônio José da Rocha, Antonio Carlos Martins
Maia Jr, and Suzana Maria Fleury Malheiros

Contents

24.1	Introduction	554
24.2	MR Assessment of Glial Tumors	558
24.2.1	MR in Preoperative Histological Grading	558
24.2.2	The Assessment of Tumor Extension and Signs That Are Indicative of Infiltration When Using MR for Appropriate Surgical Planning	568
24.2.3	The Guidance of Stereotactic Biopsy Procedures	568
24.2.4	The Assessment of the Affection of Eloquent Areas of Brain Parenchyma	572
24.2.5	Differentiation from Other Types of Processes.....	574
24.3	The Use of PET in the Assessment of Gliomas	579
24.4	The Assessment of Other Primary CNS Tumors	584
24.4.1	The Assessment of Infratentorial Tumors....	584
24.4.2	Primary CNS Lymphoma.....	589
24.4.3	The Assessment of Secondary CNS Tumors	593
	References	599

Abbreviations

[18F] FDG	2-[18F] fluoro-2-deoxy-D-glucose
[18F] FLT	[18F]fluorothymidine
[18F]FAZA	[18F]F-fluoroazomycin arabioside
[18F]FMISO	[18F]fluoromisonidazole
ACRIN	American College of Radiology Imaging Network
ADC	Apparent diffusion coefficient
ADCmin	Minimum apparent diffu- sion coefficient
AIDS	Acquired immunodeficiency syndrome
ASL	Arterial spin labeling
AT/RT	Atypical teratoid rhabdoid tumor
BBB	Blood-brain barrier
BOLD	Blood oxygen level-dependent
CBTRUS	Central Brain Tumor Registry of the United States
Cho	Choline
CNS	Central nervous system
Cr	Creatine
CSF	Cerebrospinal fluid
CT	Computerized tomography
DCE MR imaging	Dynamic contrast-enhanced MRI
DNA	Deoxyribonucleic acid
DSC MR imaging	Dynamic susceptibility con- trast-enhanced MR imaging

A.J. da Rocha, MD, PhD (✉)
A.C.M. Maia Jr, MD, PhD
Division of Neuroradiology Fleury Medicina
Diagnostica, Faculdade de Ciências Médicas
da Santa Casa de São Paulo (FCMSCSP),
São Paulo, SP, Brazil
e-mail: a.rocha@uol.com.br

S.M.F. Malheiros, MD, PhD
Department of Neurology and Neurosurgery
(UNIFESP), São Paulo, SP, Brazil

Division of Neurology, Hospital Israelita Albert
Einstein (HIAE), São Paulo, SP, Brazil

DTI	Diffusion tensor imaging
DWI	Diffusion-weighted imaging
FET	O-(2-[18F] fluoroethyl)-l-tyrosine
FLAIR	Fluid-attenuated inversion recovery
FSE	Fast spin-echo
Gd	Gadolinium
Glx	Glutamine/glutamate
Ki-67	Index of mitotic activity
Lac	Lactate
Lip	Lipids
MET	[11C]methionine
MinIP	Minimum-intensity projection
MRS	Proton magnetic resonance spectroscopy
MS	Multiple sclerosis
NAA	<i>N</i> -acetylaspartate
PET	Positron emission tomography
PNET	Primitive neuroectodermal
PWI	Perfusion-weighted imaging
rCBV	Relative cerebral blood volume
ROIs	Regions of interest
rTBV	Relative tumor blood volume
RTOG	Radiation Therapy Oncology Group
SWI	Susceptibility-weighted imaging
T1-WI	T1-weighted imaging
TDL	Tumefactive demyelinating lesion
TE	Echo time
TSE	Turbo spin-echo
VEGF	Vascular endothelial growth factor
WHO	World Health Organization

Central nervous system (CNS) tumors are relatively rare, and their diagnosis, therapeutic management, and follow-up represent challenges. However, the various available imaging methods no longer provide exclusively descriptive anatom-

ical information. Advanced imaging techniques now allow for the assessment of functional parameters, thus maximizing the potential of these techniques for diagnosis and treatment assessment. In the present chapter, we discuss the role of these techniques in the diagnosis and treatment planning of CNS neoplasms. In addition, we describe the main features of intra-axial primary and secondary neoplasms as well as their differentiation from nonneoplastic, space-occupying lesions.

24.1 Introduction

Primary CNS tumors are relatively rare. According to epidemiological data from the Central Brain Tumor Registry of the United States – CBTRUS, the estimated incidence of new cases of primary CNS tumors will be 69.720 in 2013, with 24.620 of these tumors being malignant [1, 2].

According to the American Cancer Society [3], primary CNS tumors are among the ten most deadly neoplasms, corresponding to 13.700 deaths/year [4]. The incidence of newly diagnosed cases is 20.6/100.000 inhabitants/year, of which 7.3/100.000 correspond to malignant tumors. The rate of new cases increases to 26.8/100.000 inhabitants/year when only the adult population (>20 years of age) is taken into account. The estimated prevalence of malignant CNS tumors is 61.9/100.000 inhabitants [4]. For reasons that are not yet fully elucidated, the elderly population exhibits a higher incidence of malignant gliomas.

Imaging studies play a major role in the *in vivo* diagnosis of CNS neoplasms. Among the various methods, MRI has the widest clinical applicability due to its availability and cost-benefit ratio. MR imaging allows for the characterization of lesions on the grounds of the structural modifications that are induced in the affected tissues, specifically, the architectural distortion (anatomical change) caused by their greater water content (T1-hypointense signal/T2 fluid-attenuated inversion recovery (FLAIR) hyperintense signal) or the replacement of tissue by a heterogeneous content with variable cellularity, blood, or necrosis. Image-based diagnoses of structural lesions must establish their topography, dimensions,

mass effect, degree of peritumoral vasogenic edema, and enhancement by the paramagnetic contrast agent (gadolinium – Gd).

Image-based diagnoses of brain structural lesions are based on the combination of space occupation and parenchymal infiltration, whereby analysis of MR images may often indicate the predominance of infiltrative or expansive characteristics. Predominantly infiltrative lesions are necessarily intra-axial, and the signal alteration is enmeshed within normal tissue, resulting in little anatomical damage (less architectural distortion), with little or no mass effect/vasogenic edema. This type of lesion is generally more indolent and usually manifests itself by the dysfunction of the affected tissue or area, often resulting in epileptic seizures rather than neurological deficits. Predominantly expansive lesions, in turn, are characterized by greater parenchymal destruction and mass effect. Consequently, these masses result in greater architectural distortion, as the tumor replaces the normal tissue, adopts variable configurations, and is generally associated with greater vasogenic edema and mechanical compression, resulting in variable degrees of intracranial hypertension and frequent neurological deficits.

Conventional MR sequences also allow for the monitoring of the modifications induced by both surgical and conservative treatment, as well as the consequences of adjuvant chemotherapy and/or radiotherapy. However, it is worth noting that conventional sequences exhibit significant limitations. The morphological characteristics of glial tumors in conventional MR sequences do not provide a reliable basis for the unequivocal histological diagnosis and do not establish the grade of malignancy [5, 6]. Additionally, although the disruption of the blood–brain barrier (BBB) is generally considered to be indicative of malignancy in glial tumors, this disruption does not provide an accurate prediction of the histological grade of the tumors, especially considering that 20 % of low-grade gliomas present enhancement by Gd, whereas as many as 40 % of anaplastic gliomas may lack Gd enhancement [7–9].

The most common primary CNS tumors are of neuroepithelial origin, and 29 % of

such neoplasms are gliomas [1], including astrocytomas, oligodendrogliomas, and mixed gliomas (oligoastrocytomas), among others. In addition, the largest series of intracranial masses described in the literature point to the relevance of other differential diagnosis, including secondary neoplasms (8 %), CNS lymphomas (2.2 %), and nonneoplastic diseases, such as tumefactive demyelinating lesions (3 %), vascular lesions (2 %), and abscesses (1 %) [1].

The diagnosis of the various subtypes of CNS tumors is based on anatomical-pathological paradigms that demand the collection of tissue samples to establish the tumor's predominant cell type, the cellular arrangement, and the expression of defined immunohistochemical markers. As molecular genetic markers have recently been included in the pathological diagnosis of the CNS tumors and as certain tumors may be heterogeneous (e.g., diffuse gliomas, and pineal tumors), the pathological diagnosis depends on the area of the material that is assessed by the pathologists [10]. Although thorough MR imaging analysis cannot provide a presumptive diagnosis that is able to replace the anatomical-pathological paradigms in force, this type of imaging is useful to identify the most appropriate areas for biopsy and to provide data regarding the biological behavior of tumors. These data can then be added to histopathological (cell) data that are derived from microscopy samples. In vivo macroscopic analysis by means of conventional MR sequences must establish several characteristics of the images, such as infiltration versus space occupation, the presence of calcifications, cysts, hemorrhage, or necrosis. These evaluations must also include a thorough analysis of the integrity of the BBB following an intravenous injection of a paramagnetic contrast agent. Due to the technological advancements that have been achieved in previous decades, MR studies no longer provide exclusively anatomical (structural) assessments but have also become a potential tool to also assess certain functional parameters. Therefore, the nonconventional images that can be acquired in variously weighted sequences are considered alongside data from conventional sequences, allowing for the in vivo analysis

of other biological and biochemical tumor characteristics, such as the assessment of tumor cellularity; the analysis of the integrity, displacement, or infiltration of white matter tracts; the assessment of the dynamic susceptibility to the passage of gadolinium through the microvascular bed based on the BBB permeability and capillary density; and the biochemical analysis of live tissue [11]. The application of cortical mapping using MR techniques with blood-oxygen-level-dependent (BOLD) imaging has also been recommended as noninvasive alternative for the preoperative planning of lesions affecting eloquent areas.

The proper application of the available imaging-based diagnostic techniques should not seek to establish the histological diagnosis of CNS neoplasms, which requires invasive methods, but to provide additional parameters that are useful in the selection of the most representative areas for pathological diagnosis, postoperative follow-up, and the assessment of the response to chemotherapy [12, 13]. In addition to the basic standard protocol of conventional sequences, we recommend the addition of advanced MR imaging techniques to include the analysis of relevant physiological data in the diagnosis and classification of CNS neoplasms (Table 24.1) [5].

Although high-field MRI (3 T) provides images with better quality, 1.5 T devices are more widely available and well accepted therefore, the limits of image interpretation are well known. The use of intravenous paramagnetic contrast (Gd) is mandatory in the absence of specific contraindications. The acquisition of delayed images (approximately 20 min) associated with a greater Gd concentration (0.3 mmol/kg), which is required to perform perfusion-weighted imaging (PWI), has been recommended to ensure greater lesion detection [11].

The combined information provided by applying conventional and functional MR sequences represents the best approach for the estimation of the histological grade, especially in the case of diffuse gliomas, as well as for the differential diagnosis between primary and secondary neoplasms [15]. Moreover, imaging-based diagnosis

Table 24.1 The standard protocol for brain tumor imaging based on expert panel discussions (primarily from ACRIN and RTOG) [11, 14]

Standardized MR imaging protocol

Three-plane localizer/scout (in order of acquisition)
 T1-weighted precontrast (spin-echo)
 T2-weighted axial
 FLAIR (optional to perform following contrast)
 T1 map (quantitation) for DCE MR imaging — 3D gradient-echo T1 or 2D TSE/FSE T1
 DWI and/or DTI (can extract DWI data trace/ADC from DTI)
 T2* DSC MR imaging (following presaturation DCE MR imaging sequence)
 T1-weighted postcontrast (spin-echo)
 Functional language, auditory, visual, motor testing, and MRS
 Can perform FLAIR prior to DSC MR imaging, SWI T2*, and additional optional sequences

General parameter recommendations

Section thickness ≤ 5 mm
 Delay is recommended, which can be built in by performing DWI and/or DTI prior to acquiring the T1 sequences. Another option is to perform FLAIR (or even T2) prior to the T1 sequences, potentially conferring additional sensitivity for leptomeningeal diseases
 Target duration ≤ 30 min (maximum, 1.5–2.0 h)

Note: *ACRIN* American College of Radiology Imaging Network, *RTOG* Radiation Therapy Oncology Group

must also take into account possible differential diagnoses, identify the primary patterns of pseudotumoral lesions, and contribute to the indication and better use of biopsy procedures (Table 24.2) [5, 16].

Although MRI is the first-choice technique for the identification of CNS neoplasms, its use is not always possible. Under such conditions, computerized tomography (CT) with intravenous iodinated contrast is a noninvasive technique that can provide information regarding the tumor vessels and angiogenesis (perfusion CT). This technique exhibits a satisfactory correlation with the histology and is of some relevance to the classification and prognosis of neoplasms [17].

Hereafter, the application of functional MR sequences in the characterization of the different patterns of the main primary and secondary intra-axial neoplastic processes will be discussed, as will their most relevant differential diagnoses.

Table 24.2 Functional MR techniques – primary applications and findings in the assessment of CNS neoplasms and their differential diagnosis

	DWI	Perfusion T2 – DSC-MRI			Perfusion T1 – DCE-MRI	Spectroscopy
Main applications	The assessment of cell density and nuclear-cytoplasmic ratio	The assessment of the microvascular density			The assessment of the integrity of the blood-tumor barrier	In vivo biochemical tissue assessment
	The assessment of signs of displacement and the invasion of white matter tracts	Tumor histological grading	Tumor histological grading			The assessment of the tumor cell density and cell multiplication rates
	The characterization of the content of cystic/necrotic lesions	Differentiation between high-grade lesions and inflammatory-based processes	Differentiation between high-grade lesions and inflammatory-based processes			The characterization of signs of necrosis and anaerobic metabolism
Parameters	DWI	Minimum ADC	ADC ($\times 10^{-3}/\text{mm}^2/\text{s}$)	ADC ratio (neoplastic tissue/normal parenchyma)	Guidance of directed biopsy procedures	Differentiation between neoplastic and infectious processes
			rTBV		Enhancement curve	Cho/NAA
High-grade gliomas	Hypo --> Hyper	Hypo --> Hypo	0.75–0.96	1.28–1.68	Increased, with fast-rising curve	Increased
	Hyper	Hypo	0.51–0.63	0.83–1.15	Increased, with fast-rising curve	Increased
					Increased, with fast-rising curve	Increased
Metastases	Hypo --> Hyper	Hyper	0.68–2.2	Homogeneous	Increased, with fast-rising curve	Increased
	Hyper	Hypo	0.7	Homogeneous	Slightly increased, without fast rise	Increased
Tumefactive demyelinating lesions	Hyper in the acute phase	Hypo in the acute phase			Slightly increased, without fast rise	Increased
						Increased
						Cho/Cr
						Lip/Lac
						3.02–4.12
						2.05–3.12
						1.84–4.56
						1.48
						Increased
						Present
						Present
						Present
						Present

24.2 MR Assessment of Glial Tumors

The current classification system of CNS tumors proposed by the World Health Organization (WHO) aims to standardize the nomenclature on the grounds that the biological behavior of tumors correlates with their cell type. As this system is further able to make prognostic estimates and to indicate the best therapeutic options for certain subtypes of neoplasms, it provides a standardized classification of human tumors that is accepted worldwide. This fact is important, as without a clear definition of histopathological and clinical diagnostic criteria, epidemiological studies and clinical trials could not be conducted beyond the restricted limits of institutions [18].

The histological heterogeneity is a crucial feature in the classification of glial tumors. Although the anaplastic characteristics of gliomas are generally diffuse, the occurrence of intersperse high- and low-grade areas or mixed-cell subtypes (astrocytoma versus oligodendroglioma) in different tissue samples of a single tumor is not rare [19]. Therefore, the diagnosis of mixed gliomas also poses a challenge and is directly correlated with the representativeness of the analyzed tissue sample. Thus, a diagnosis based on stereotactic biopsies should be interpreted with caution due to the potential risk of sampling errors.

In regard to preoperative assessment, in addition to corroborating clinical suspicions based on the findings of conventional images, the primary applications of functional MR methods are as follows:

- Preoperative histological grading
- The assessment of tumor extension and signs that are indicative of infiltration for appropriate surgical planning
- Guidance in stereotactic biopsy procedures
- The assessment of the affection of eloquent areas of brain parenchyma
- Differentiation from nonneoplastic lesions

24.2.1 MR in Preoperative Histological Grading

According to the current WHO classification system, grade I tumors exhibit low proliferative

potential and may be cured following surgical resection alone. Grade II tumors are generally of infiltrative nature, and relapse often occurs following surgery despite their low proliferative activity. Certain grade II tumors tend to progress into higher grades of malignancy, e.g., low-grade (grade II) diffuse astrocytomas that may become anaplastic astrocytomas and glioblastomas. Moreover, oligodendrogliomas and oligoastrocytomas may undergo similar transformations. WHO grade III corresponds to tumors with histological evidence of malignancy, including nuclear atypia and greater mitotic activity. As a rule, patients with grade III neoplasms undergo adjuvant radiotherapy and/or chemotherapy. Lastly, WHO grade IV corresponds to malignant neoplasms with a high mitotic index, the presence of necrosis, and a greater proclivity to early relapse and death (e.g., glioblastomas) [18].

The current classification system of CNS neoplasms (WHO 2007) derives from accumulated neuropathological and genetic experience, with clinical and in vivo imaging associations [18]. Nevertheless, MRI is the preferred technique in everyday practice for the diagnosis, planning, treatment, and follow-up of patients with CNS neoplastic lesions [11]. Several imaging characteristics have been suggested as predictors of high grade of malignancy in human gliomas, including heterogeneous signal, the occurrence and pattern of contrast enhancement, the presence of mass effect, the occurrence of cysts, hemorrhaging, or necrosis, as well as the tumor metabolic activity and blood volume. Some patterns of the combination of conventional (particularly post-Gd, T1-weighted (T1W1)) and advanced functional MR imaging provide a structural, metabolic, and physiological assessment of the affected brain area. These data provide neuroradiologists, neuro-oncologists, neurosurgeons, oncologists, and radiotherapists with a practical interpretation of MR results, particularly in the case of diffuse gliomas in adults.

Despite technological advances and the optimization of MR sequences and protocols, the histological grading of diffuse gliomas based exclusively on the interpretation of MR images is unreliable as the sensitivity of the conventional sequences varies from 55–88 % [5]. Uncertainty

as to the histological grade at a given time point in the assessment of this spectral disease is even greater due to the lack of definition of the imaging factors that alter its nature. The difficulty is even greater in the absence of signs that are suggestive of biological aggressiveness, such as macroscopic necrosis or Gd enhancement. Under such circumstances, it is not possible to exclude anaplasia. Gd enhancement is not exclusive to high-grade tumors but may occur in as many as one-third of grade II gliomas and even in circumscribed gliomas (grade I). In this context, the use of functional sequences has been recommended, not to replace histopathology, which is indispensable, but as a complementary interpretative tool that may contribute to therapeutic decision making and, ultimately, to the final diagnosis [13].

Studies of glial tumors using proton magnetic resonance spectroscopy (MRS) typically reveal a reduction in *N*-acetylaspartate (NAA, 2.0 ppm) peaks and ratios, which reflects the neuronal loss and dysfunction resulting from the replacement of normal by neoplastic tissue. During preparation for cell division, at the various stages of the cell cycle, phospholipids accumulate, especially phosphatidylcholine, which constitutes approximately 40 % of the cell membrane. Choline-containing metabolites are detected using MRS (Cho, 3.2 ppm), and an increase in the choline peak and ratios is a marker of cell membrane proliferation, indicating the presence of a neoplastic process and directly correlating with the tumor cell density. Additionally, the levels of lipids (Lip, 0.9–1.33 ppm) and lactate (Lac, 1.3 ppm) may increase as a function of cell death and necrosis and the presence of anaerobic metabolism, respectively. The presence of lactate must be confirmed using MRS acquisition with an intermediate echo time (TE) (136–141 ms), resulting in the elimination of the majority of the lipid peak and reversing the lactate peak below the baseline (i.e., the J-coupling effect). These variations are more exacerbated for higher histological grade diffuse gliomas.

Metabolic ratios are known to exhibit very large variations even within a single lesion in relation to the histological heterogeneity characteristic of diffuse gliomas. Therefore, cutoff values cannot be established for the metabolic

ratios, which would allow for the unequivocal grading of glial lesions. Previous studies have shown a sensitivity of 79 % and a specificity of 85 % [20]. Nevertheless, it is worth noting that a high spectral Cho/NAA ratio – above 2.2 – indicates greater odds of high-grade lesions.

The presence of elevated lipid peaks may also contribute to this analysis as they do not occur in low-grade tumors but are typical of high-grade tumors due to cell death and necrosis and may be observed in glioblastomas [20–22]. High myoinositol peaks are also relevant findings as they are characteristic of low-grade tumors and *gliomatosis cerebri*. Low-grade diffuse glial neoplasms, particularly those involving the astrocytic lineage, may exhibit a predominant increase in myoinositol or myoinositol/glycine (3.5–3.7 ppm) values without an apparent increase in the choline/creatine (Cho/Cr) ratio. Normal or slightly increased choline levels in low-grade tumors are most likely due to the low cell division rates of such lesions. In addition, the reduced production of proteolytic enzymes and a low rate of cell destruction may account for the predominant increase in the myoinositol peaks in low-grade tumors (Fig. 24.1). Although *gliomatosis cerebri* corresponds to WHO grade III, its characteristics on conventional images are sufficiently clear to distinguish it from grade II gliomas, characterized by an exceptionally extensive infiltration with the involvement of at least three cerebral lobes, usually with bilateral involvement of the cerebral hemispheres and/or deep gray matter and frequent extension to brain stem, cerebellum, and spinal cord according to the WHO definition [23].

Tumor growth, which is associated with high multiplication rates and cell turnover, increases the metabolic demands in neoplasms. Cell hypoxia and hypoglycemia elicit the production of angiogenic cytokines, such as the vascular endothelial growth factor (VEGF), which induce the formation of new blood vessels that characterizes tumor angiogenesis [24, 25]. The increase in capillary density results in increased blood flow and volume in the tumor bed [24]. Angiogenesis results in the formation of a complex network of anomalous vessels in the peritumoral area. Susceptibility-weighted imaging (SWI) is a

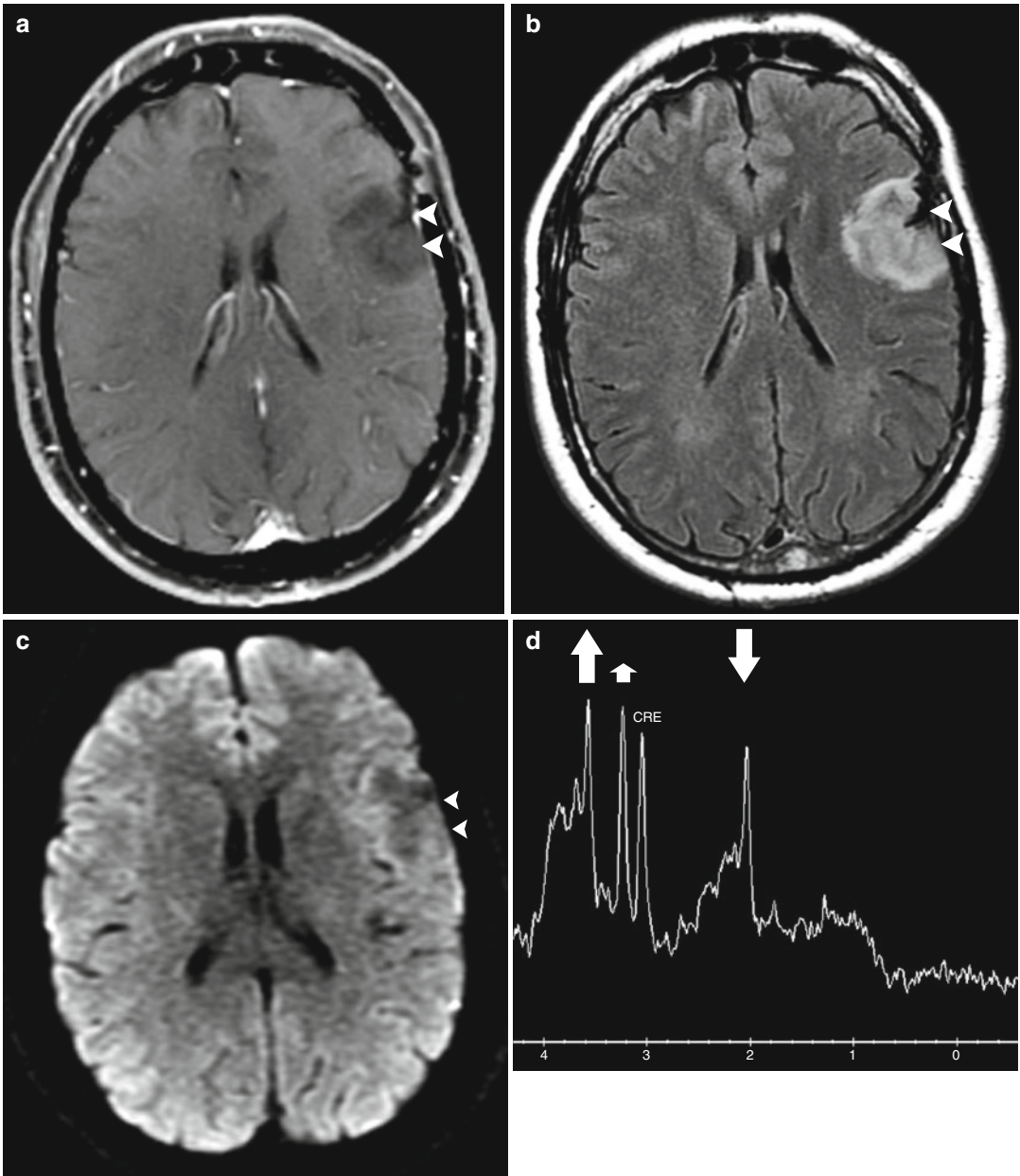


Fig. 24.1 Low-grade astrocytoma (WHO grade II). Comparative follow-up axial images on T1WI (a), FLAIR (b), and DWI (c) showed an infiltrative cortical and sub-cortical tumor in the inferior frontal gyrus (arrows), without Gd enhancement. MRS (TE = 31 ms) (d) confirmed a reduced NAA peak (downward arrow), associated with high myo-inositol (upward arrow) and only minimally increased choline peak (small upward arrow). DSC-MRI (e) demonstrated diffuse low rTBV. Dynamic susceptibility

curves (f) from the lesion (purple lines) resulted similar to the normal contralateral white matter (green line). Imaging follow-up after 3 years with comparative axial plane FLAIR image (g) confirmed a tumor enlargement (arrowheads), with identical DSC-MRI (h) results. Comparative MRS (i) showed an even more reduced NAA peak (downward arrow) associated with elevated choline (small upward arrow) and unaltered myo-inositol (upward arrow). A small lesion on right superior frontal gyrus (arrowhead on g) was attributed to the history of seizure with previous head trauma (gliosis)

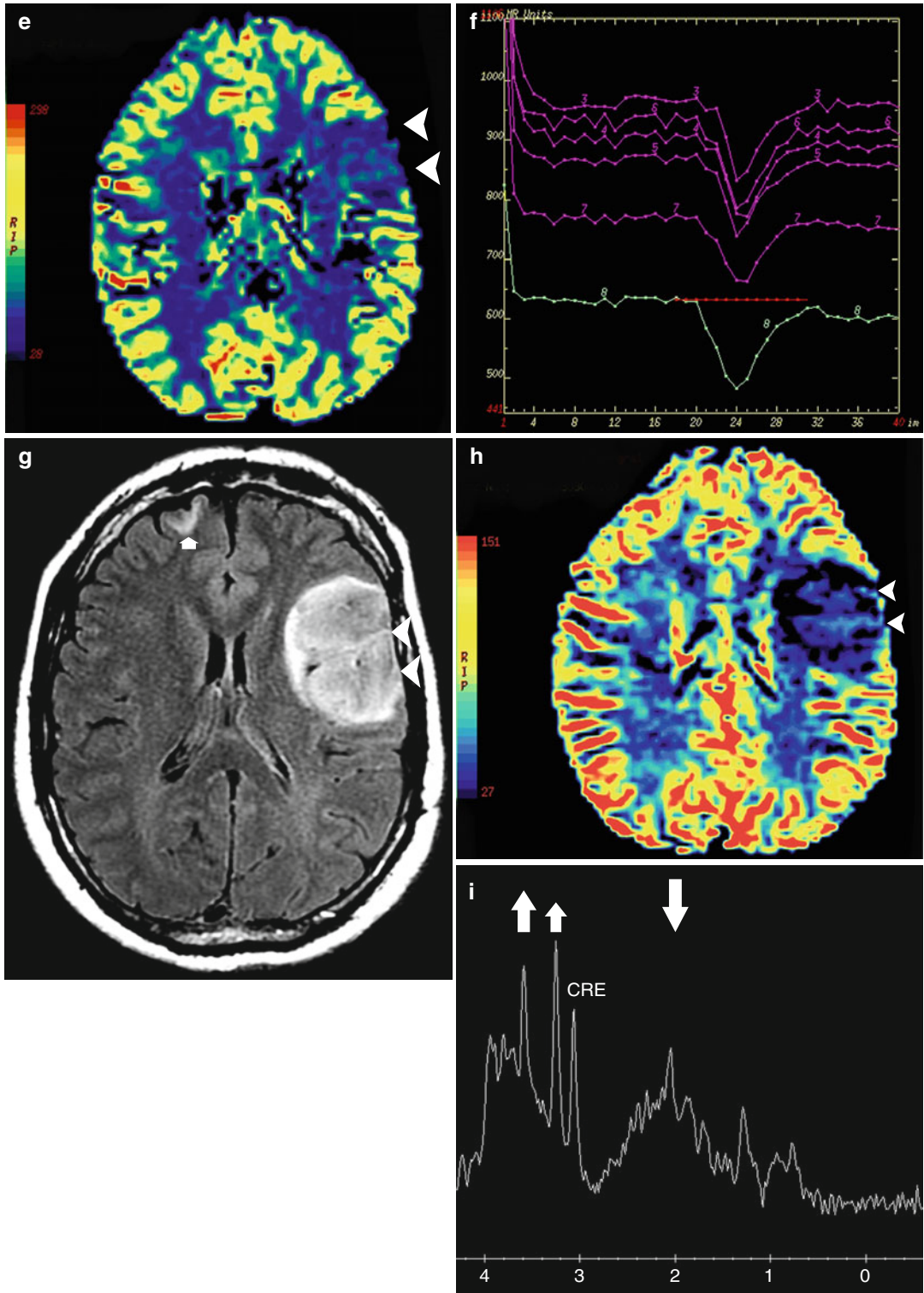


Fig. 24.1 (continued)

novel MR technique that is based on the different magnetic susceptibility of tissues. Multiplication of the phase images by the magnitude images makes the small veins more conspicuous, as well as other sources of susceptibility effects, which are demonstrated using a minimum-intensity projection (MinIP). The unique ability of SWI to demonstrate a T2* effect, as well as the possibility of making evident the presence of tumor neovascularization, makes it a useful technique in the study of brain tumors (Fig. 24.2) [26].

Histological studies show that tumor vessels are immature and highly permeable due to large spaces between the endothelial cells, incomplete basement membrane, and a lack of smooth muscle layer. The released cytokines may also exert a modulatory effect on the increase in vascular permeability [24]. Tumor cells may also cause direct damage to the BBB, which may result in increased vascular permeability [27]. Tumor blood vessels are more tortuous, which may increase the distance the gadolinium molecules must travel inside of the lesion and, consequently, the mean transit time of the blood in the tumor bed. As a consequence of the association of these factors, increased relative tumor blood volume (rTBV) and vascular permeability is the typical finding when using dynamic susceptibility contrast-enhanced MR imaging (DSC-MRI) and is directly correlated with the histological grade of the lesion (Fig. 24.3) [12].

T1-weighted, steady-state, dynamic contrast-enhanced MRI (DCE-MRI) and T2*-weighted, dynamic susceptibility-weighted contrast-enhanced MRI (DSC-MRI) are the two of the most widely used PWI techniques. DSC-MRI (dynamic first-pass study) is the most widely used technique, and several research groups have demonstrated its usefulness in the preoperative assessment of brain tumors [5, 20, 28, 29]. High-grade gliomas typically exhibit greater rTBV values compared to the low-grade tumors. The application of echo planar gradient echo sequences (T2* – DSC-MRI) to the study of intra-axial lesions allowed for the establishment of $rTBV \geq 1.75$ as a cutoff point for distinguishing between high- and low-grade gliomas [30]. However, it is worth noting that extravasation

of the paramagnetic contrast agent into the extravascular compartment may hinder the measurement of rTBV and thus compromise the reliability of the assessment of lesions, such as glioblastomas, which typically exhibit a loss of integrity of the blood-tumor barrier [31].

Perfusion techniques using DSC-MRI and DCE-MRI acquisitions are widely used in the assessment of glial neoplasms. Although both techniques have their advantages and disadvantages, DCE-MRI appears to be more sensitive than DSC-MRI in detecting contrast medium extravasation. The correlation values of capillary permeability with immunohistochemical markers suggest that this imaging technique is useful in the preoperative characterization of gliomas [32].

The undesirable effects of T1 signal shortening in the tissue due to interstitial extravasation of Gd have been shown on PWI sequences. Such effects may be minimized by administering 0.05–0.10 mmol/kg of the paramagnetic agent prior to the PWI acquisition [33]. The saturation of the peritumoral interstitium in areas with BBB disruption reduces the negative effects caused by Gd extravasation as a result of the alteration of the dynamic plot, which reflects the reduction in the T2 signal intensity in the analyzed tissue [34]. Therefore, we recommend administering an intravenous infusion of a small volume of Gd (approximately 5 ml in adults) for prior correction of paramagnetic agent extravasation into the tissue interstitium, thus normalizing the plot baseline of the dynamic acquisitions of MR imaging perfusion. However, a certain degree, generally small Gd extravasation may still occur, even in the case of lesions for which the conventional sequences are not enhanced (post-Gd T1W1) and for which the usual concentration of Gd (0.1 mmol/kg) is used. Therefore, the effect of T1 shortening of the tissue during the first passage of the paramagnetic agent may not be entirely excluded.

Although areas with elevated rTBV represent hypervascularized regions inside expansive tumors, it may not be possible to estimate the vascularization of each image element due to the sequence's low signal-to-noise ratio. Therefore, the calculation of the value of the relative cerebral

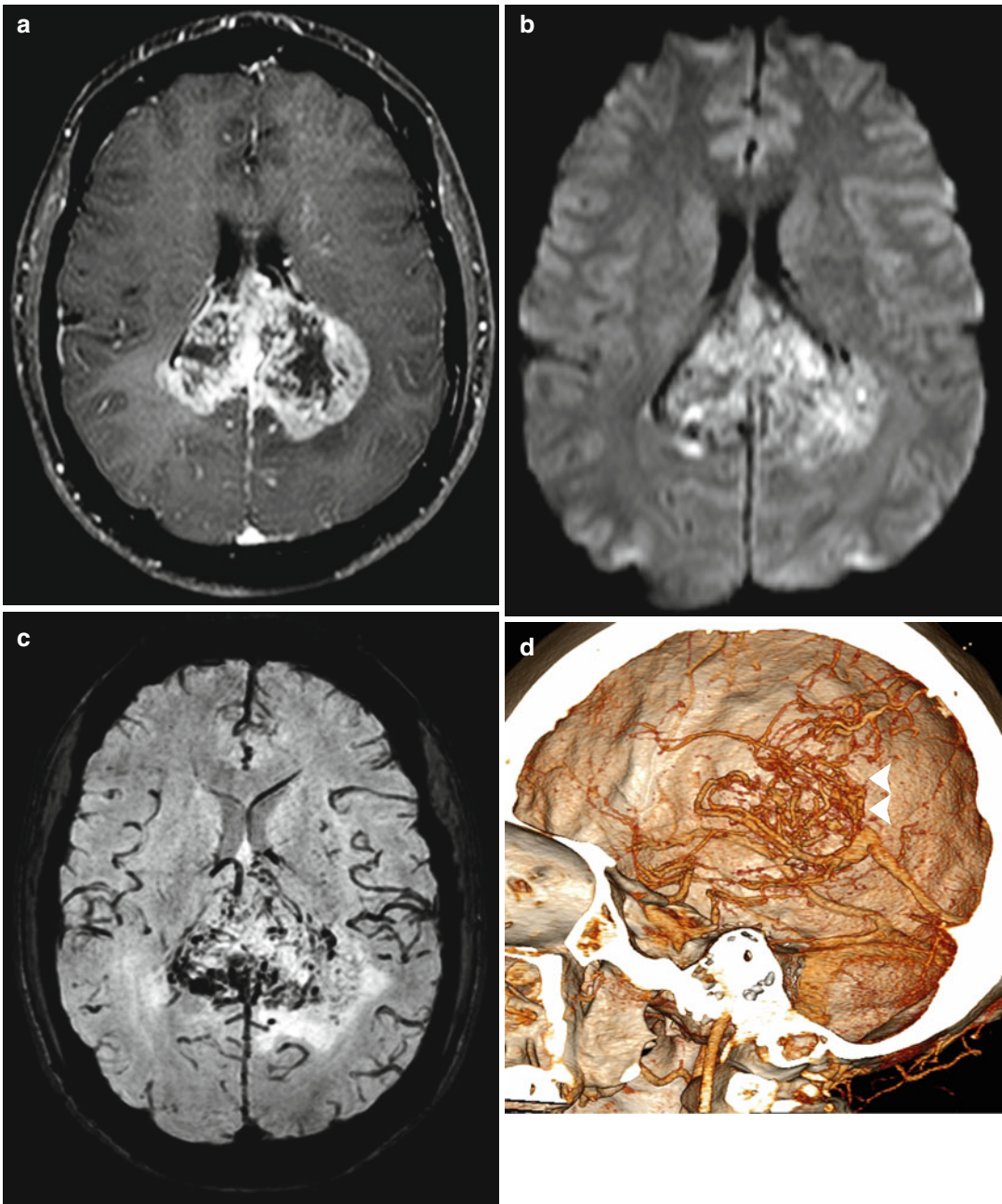


Fig. 24.2 Glioblastoma of the corpus callosum (WHO grade IV). Bilateral tumor in the splenium of the corpus callosum (“butterfly appearance”) showing an extensive necrosis on T1WI after Gd administration (**a**). Note restricted water diffusion on DWI (**b**) suggesting a hypercellular tumor. Comparative SWI acquisition (**c**) in the axial plane showed widespread vessel proliferation in the

tumor, confirmed on this computed tomography angiography 3D-reconstruction (**d**) (*arrowheads*). High capillary density and high vessel permeability were also demonstrated on DSC-MRI (**e**) and on DCE-MRI (**f**). MRS ($TE=31$ ms) (**g**) showed reduced NAA peak (2.0 ppm) associated with elevated choline (3.2 ppm), lipids, and lactate peaks (0.9–1.3 ppm)

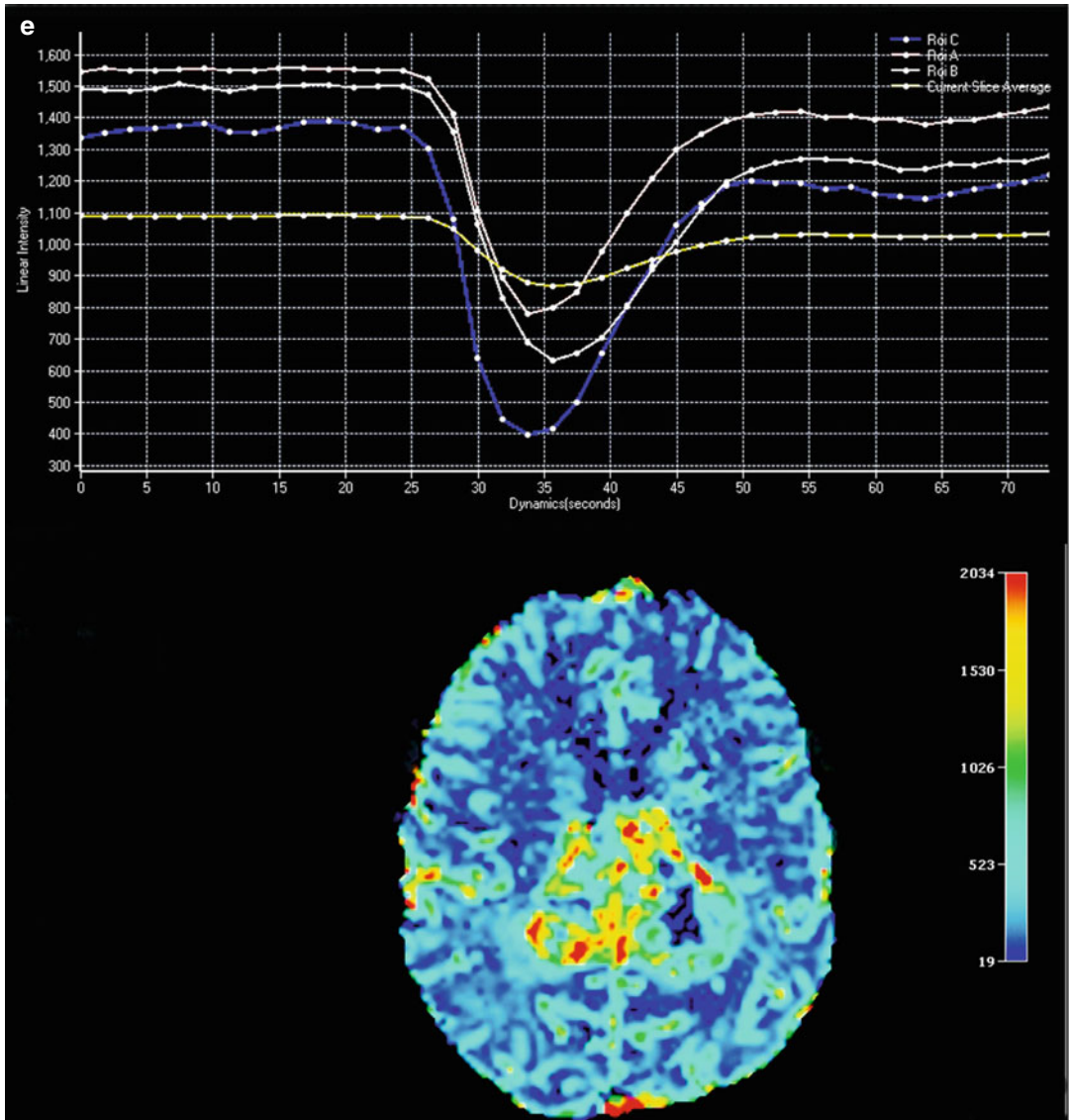


Fig. 24.2 (continued)

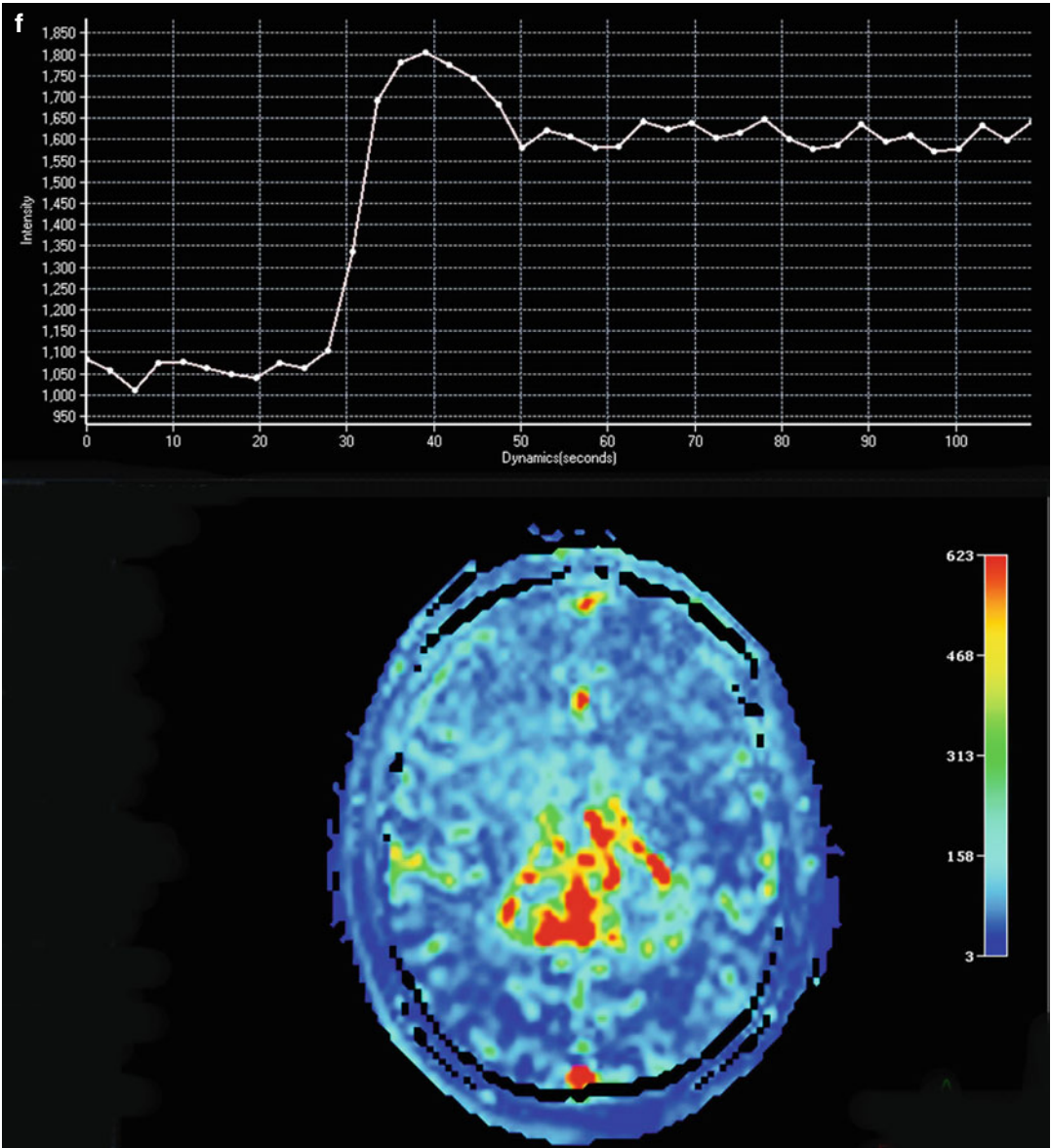


Fig. 24.2 (continued)

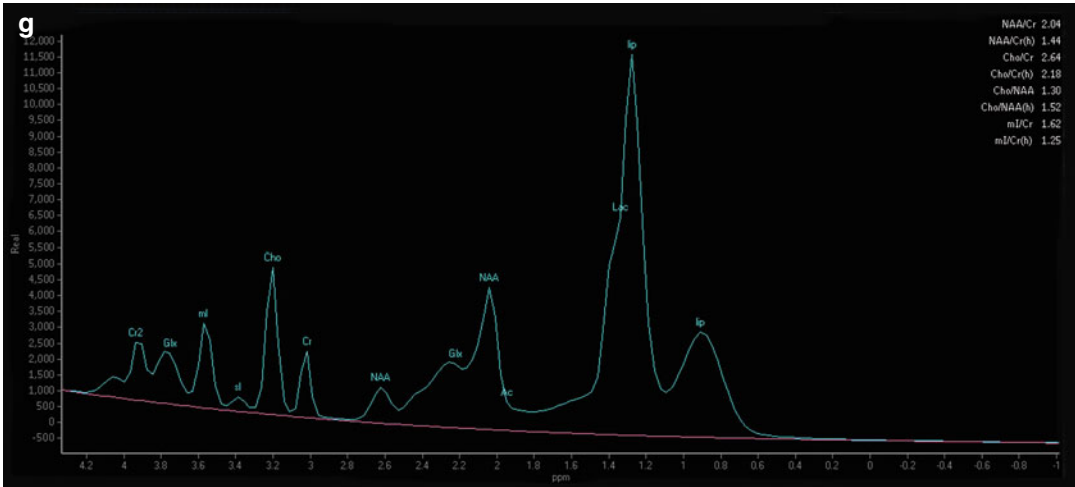


Fig. 24.2 (continued)

blood volume (rCBV) in regions of interest (ROIs) of a given brain parenchyma area is preferable. In large-sized lesions, multiple rCBV values may be measured in several ROIs. Although the size of ROIs varies as a function of the size of the lesion, ROIs with 1- to 5-mm diameters are generally used. Using this procedure, the area with greatest rCBV within a heterogeneous lesion may be easily characterized. A minimum of six measurements must be performed in different areas of interest to establish the maximum rTBV values of the tumor. This technique exhibits appropriate intra- and inter-examiner reproducibility.

The interpretation of perfusion studies of oligodendrogliomas demands extra caution given that these tumors may represent an exception to the common interpretation, as they exhibit areas with high rTBV despite their low histological grade [35, 36], especially tumors with the 1p19q codeletion [37]. This variation may be explained by the presence of a dense capillary network in oligodendrogliomas (Fig. 24.4) [35]. As oligodendrogliomas exhibit a greater tendency for cortical involvement [38], and as cortical vascular density is greater compared to that of the white matter, high cortical rTBV values may also be considered to be a possible interference in the readings or sources of diagnostic error.

Arterial spin labeling (ASL) is a novel technique to measure the blood flow that obviates the requirement for the use of intravenous contrast agents. This

novel technique became quite attractive due to the availability of repeated measures without Gd administration. A radio-frequency pulse upstream to the tumor alters the water molecules that cross the area, making their MR signal detectable. This alteration provides an absolute value for the blood flow. ASL exhibits low signal-to-noise ratio and may be more susceptible to the patients' movements. Further improvements and studies are required before it may be applied routinely in that was clinic. Nevertheless, this technique was previously demonstrated to be as sensitive as DSC-MRI in the study of gliomas [12].

Diffusion-weighted, imaging (DWI)-based MR contrast reflects the Brownian motion of the water in the analyzed tissue. An inverse correlation between the minimum apparent diffusion coefficient (ADC_{min}) and the lesion cellularity was previously confirmed by histological analysis in a wide variety of tumors, including high- and low-grade gliomas, lymphomas, medulloblastomas, meningiomas, and metastases. Gliomas are characterized by remarkable signal heterogeneity in ADC maps. Most likely due to their high cell density, the tortuosity of the interstitial space, and the hindrance to the free motion of the water molecules, the ADC values of high-grade gliomas are typically low, whereas these values tend to be lower in lower-grade tumors [39]. ADC_{min} values from 1.7 to 2.5 may be used as cutoff points to distinguish between high- and low-grade gliomas [40]. Unfortunately, there is a wide overlap in the

results of such analyses; therefore, this parameter cannot be used alone in the histological grading of glial neoplasms.

In addition to the modifications in the histopathological and genetic approach to classifying

gliomas, the fourth edition of the classification system of CNS tumors (WHO 2007) [18] lists several new entities, including angiocentric glioma, papillary glioneuronal tumor, rosette-forming glioneuronal tumor of the fourth

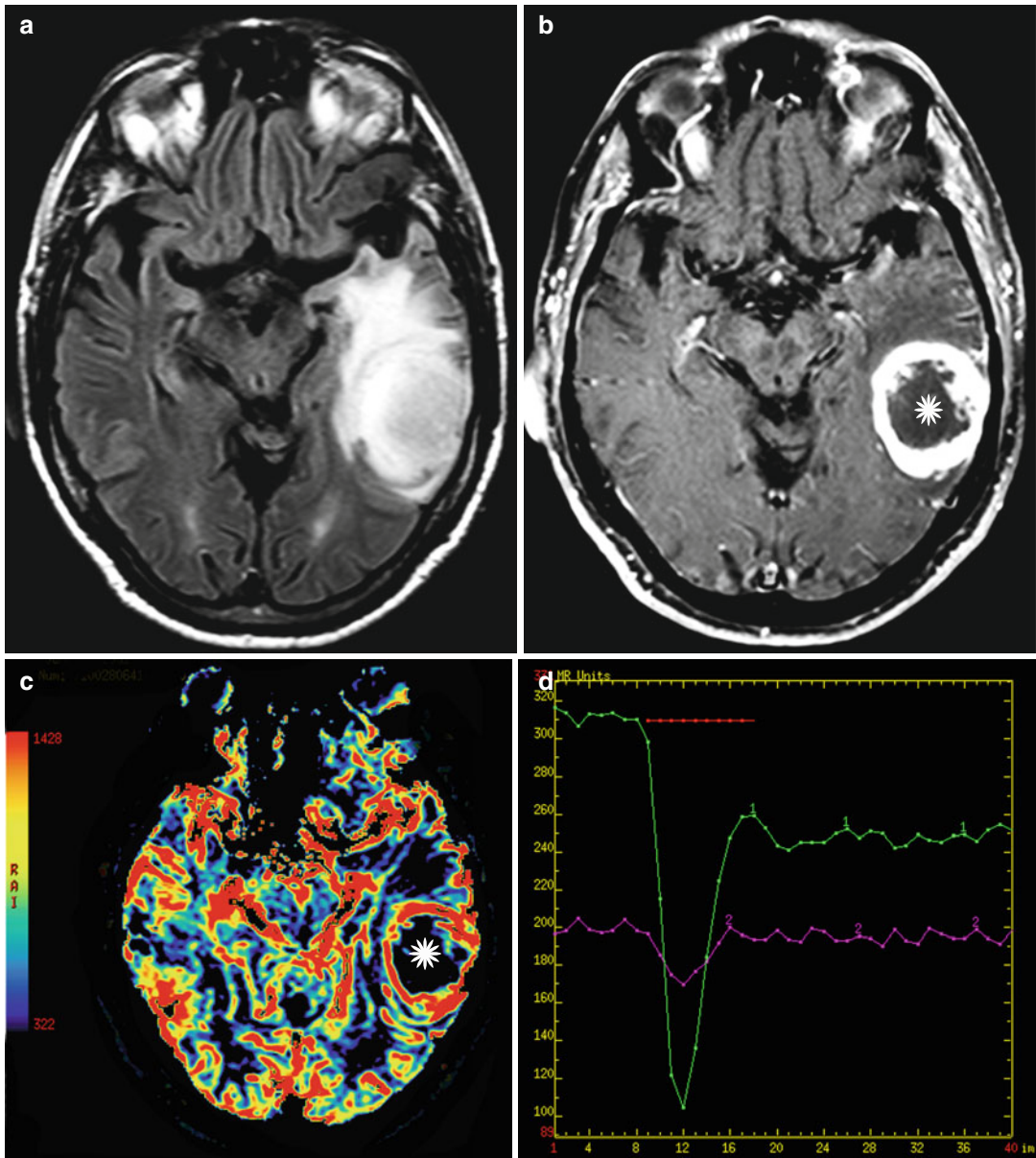


Fig. 24.3 Left temporal lobe glioblastoma (WHO grade IV). Conventional sequences demonstrated an infiltrative tumor in the left middle temporal gyrus characterized by extensive hyperintensity on FLAIR image (a) and a ring enhancement with evident necrosis (*asterisk*) on T1WI post-Gd administration (b). DSC-MRI (c) confirmed ane-

lar hyperperfusion area larger than the solid portion of the tumor. Dynamic susceptibility curve (d) from the tumor has suggested local neoangiogenesis (increased capillary density) in the tumor and high permeability on DCE-MRI (e) (*arrowheads*)

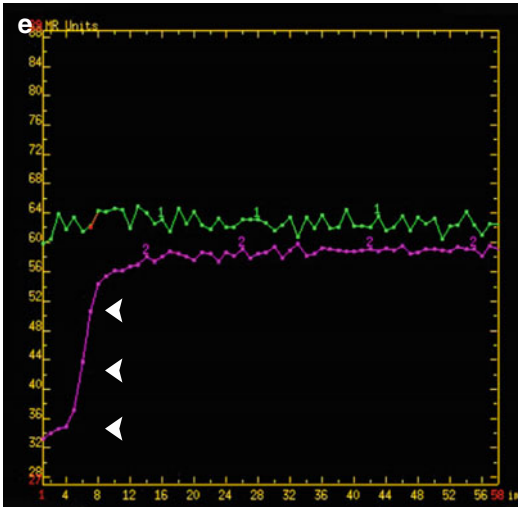


Fig. 24.3 (continued)

ventricle, papillary tumor of the pineal region, pituitaryoma, and spindle cell oncocytoma of the adenohypophysis [18]. Moreover, histological variants were also added to the previous list (pilomyxoid astrocytoma, anaplastic medulloblastoma, and medulloblastoma with extensive nodularity) whenever evidence of particularities in the age distribution, localization, genetic profile, or clinical behavior is established. The imaging patterns of the novel neoplasms and recently described variants are not fully established, as their description is based on sporadic reports or small case studies [41–46].

24.2.2 The Assessment of Tumor Extension and Signs That Are Indicative of Infiltration When Using MR for Appropriate Surgical Planning

Conventional MR sequences do not allow for the differentiation between peritumoral vasogenic edema and tumor infiltration. The growth of gliomas is characterized by the infiltration of adjacent white matter tracts; thus, the growth generally extends beyond the limits of the expansive portion of the tumor, even in those that exhibit focal or multifocal disruption of the blood-tumor barrier. Occasionally, tumors even extend beyond

the limits of the signal alteration itself identified on conventional sequences. Earnest et al. [47] demonstrated the extension of tumors not only beyond the enhanced portion on MR but also beyond the portions with T2 hypersignal. Thus, notwithstanding its paramount importance in the planning of surgery and radiotherapy, the assessment of the margins of glial tumors poses a major challenge.

The generalized infiltration of the circumjacent tissue indicates the proclivity of CNS tumors to craniospinal dissemination and is characteristic of WHO grades III and IV. The functional MR sequences may provide important information in this regard. MRS, more particularly multivoxel acquisition, may identify alterations in metabolic ratios, especially increases in the Cho/NAA ratio, beyond the limits of the enhanced areas (post-Gd T1W1). In such areas, a marked reduction in ADC and an increase in fractional anisotropy may be a useful finding and contribute to the characterization of the infiltration of large white matter tracts [48, 49].

There have been previous reports regarding the use of tractography to distinguish between the displacement, infiltration, and destruction of white matter tracts (Fig. 24.5) [50, 51]. However, the application of its parameters of interpretation to the clinical routine must be performed with caution (Fig. 24.6). It appears that the occurrence of false-positive results restricts the application of this technique to the study of individual patients; therefore, there is a gap between the clinical routine and the theoretical fundamentals and models based on patient studies.

24.2.3 The Guidance of Stereotactic Biopsy Procedures

Imaging-guided stereotactic biopsy procedures are based on the notion that tumor areas with BBB disruption, and consequent contrast medium (Gd) enhancement, correspond to neoplasm areas with higher histological grades. As mentioned above, this criterion may not be used alone to histologically grade glial tumors; as many as 40 % of gliomas without enhancement on MR exhibit

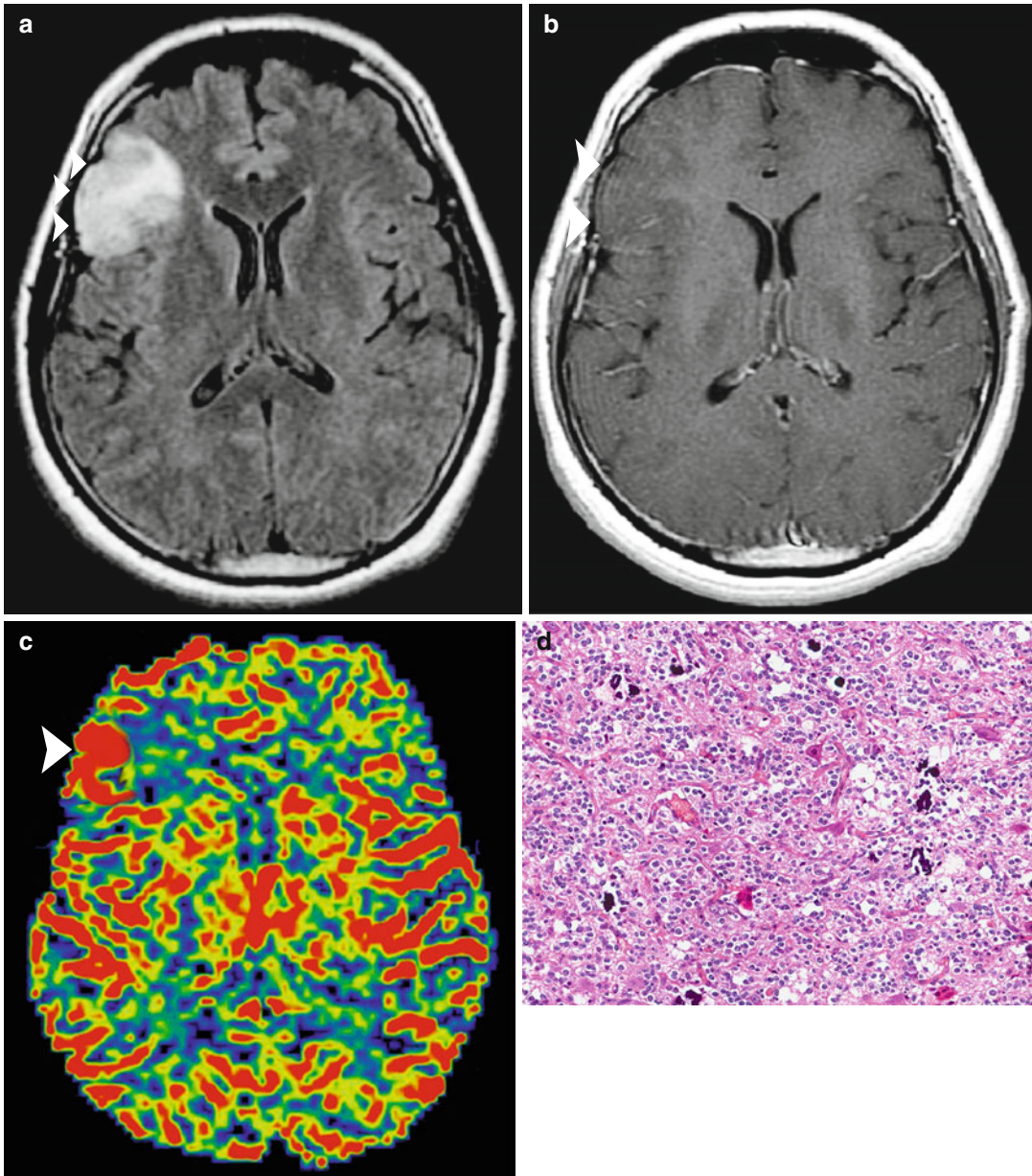


Fig. 24.4 Oligodendroglioma (WHO grade II). Comparative axial FLAIR (a) and T1WI post-Gd (b) showed a cortical tumor in the right inferior frontal lobe without contrast enhancement (arrows). DSC-MRI (c)

showed focal hyperperfusion more evident than in the contralateral similar area. Note a dense capillary network typical of an oligodendroglioma in this histopathologic study (d)

anaplasia on histological examination [52, 53]. The application of this flawed approach has been the source of sampling errors in biopsies and underestimates the histological grade of tumors.

Appropriate histological grading has paramount importance in the planning of treatment.

Patients with low-grade gliomas may be indicated for conservative treatment, with consequent lower morbidity and mortality, whereas those for which the histological grade has been overestimated may undergo unnecessary adjuvant treatments.

It is worth stressing that the histological diagnosis may pose a major challenge in a subset of patients due to their heterogeneity, i.e., diffuse

gliomas may exhibit multiple histological grades or cell subtypes. Additionally, the natural progression of low- to high-grade gliomas

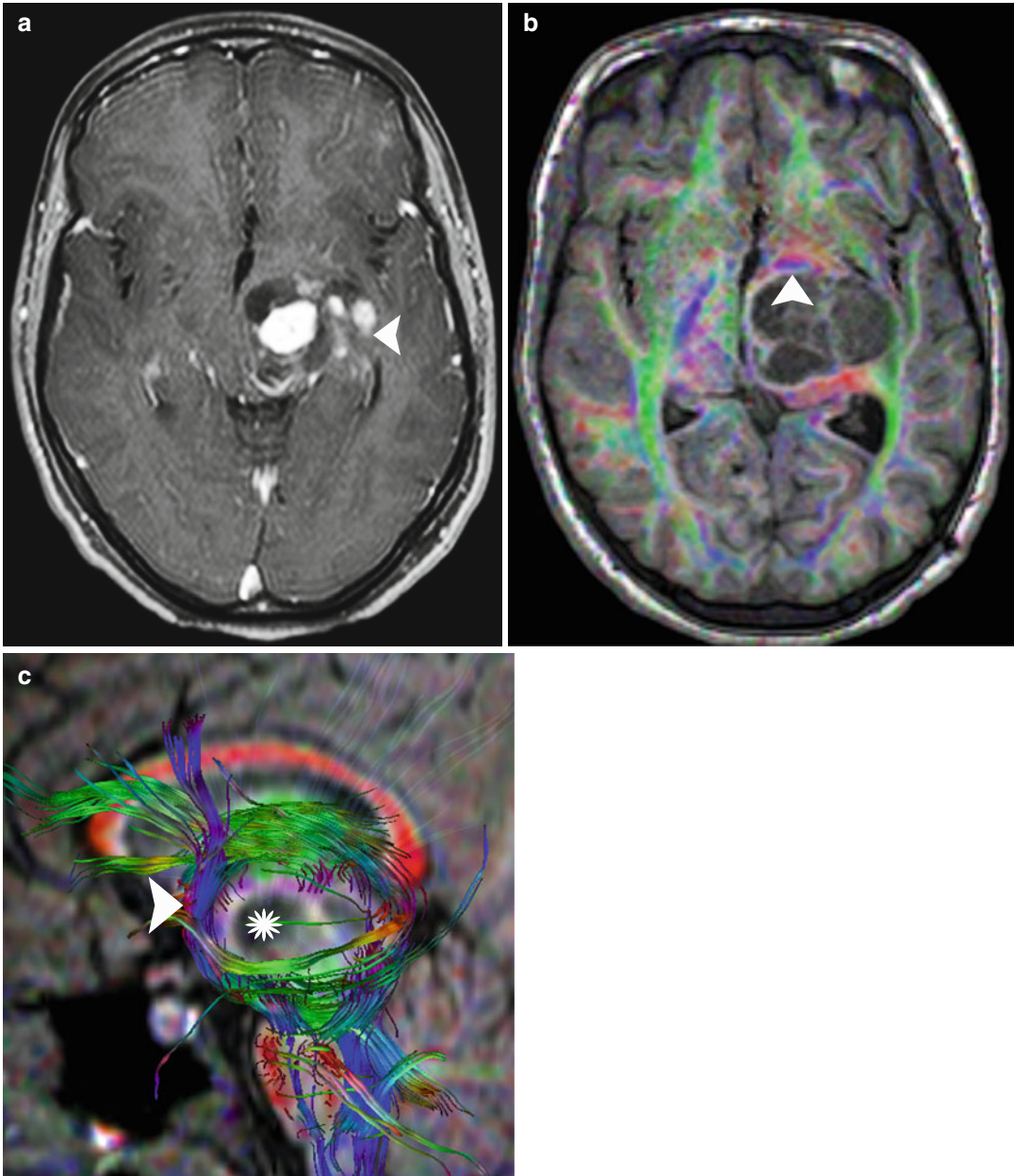


Fig. 24.5 Diffusion tensor imaging contribution to the surgical approach of a thalamic glioma. Axial T1WI post-Gd administration (a) showed a solid-cystic pilocytic astrocytoma (arrowhead). A DTI was performed to surgical planning, and directional imaging (b) demonstrates this expansive lesion (asterisk) with a predominant forward

displacement of the left corticospinal tract (arrowhead), confirmed on tractography (c). MRS with short TE (d) and long TE (e) showed reduced NAA peak (2.0 ppm) associated with elevated choline (3.2 ppm) and lactate peaks (1.3 ppm). Note J-coupled effect with inverted peaks of lactate on MRS with intermediate TE (141 ms) (e)

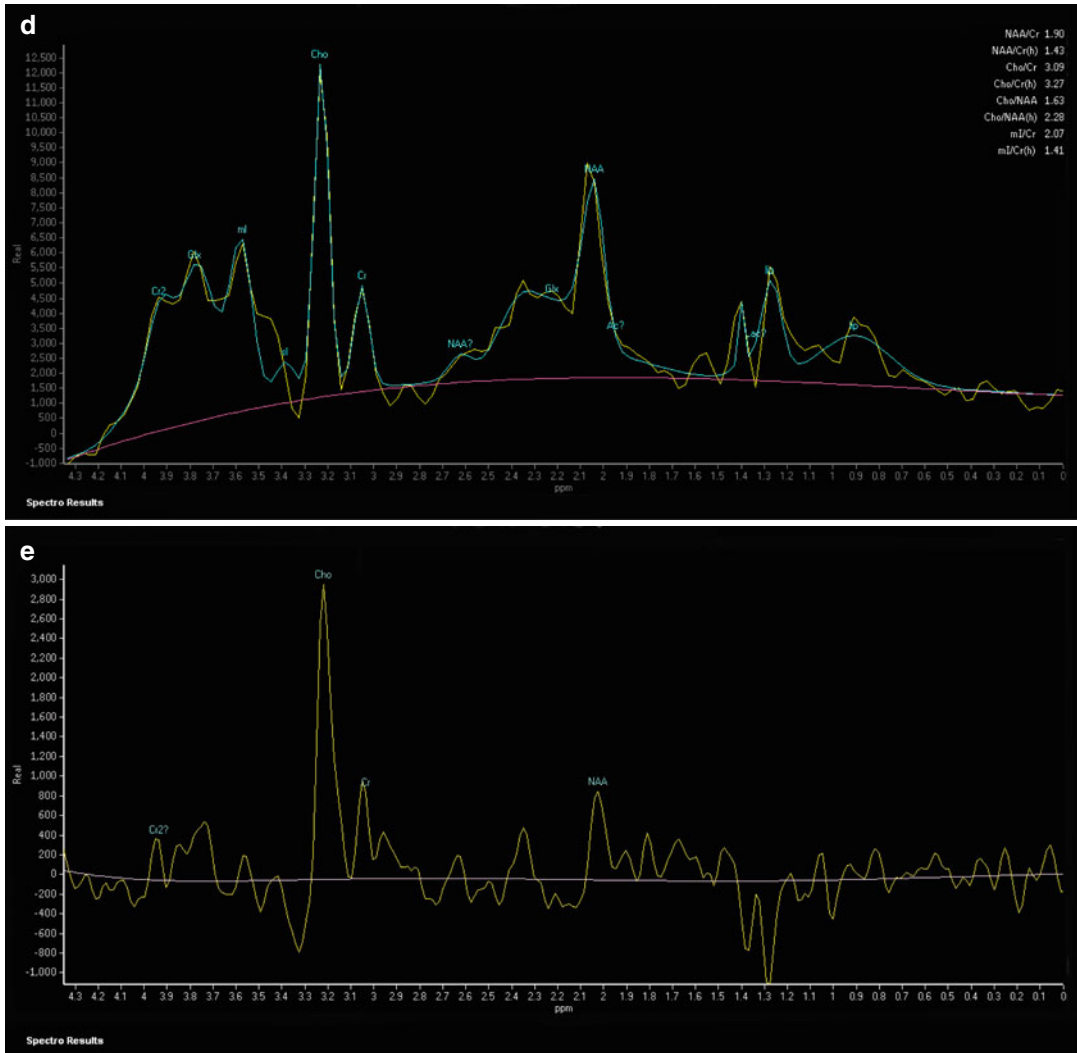


Fig. 24.5 (continued)

is not uncommon and may occur initially in focal areas, accounting for the sampling errors that occur when diagnosis is exclusively based on stereotactic biopsy with random or targeted collection of samples from Gd-positive areas [54, 55].

PWI (DSC-MRI) is the most useful among the functional MR sequences, given that it may add further information to that provided by conventional imaging, allowing for the characterization of areas with high rTBV, even in the absence of Gd enhancement. DSC-MRI is the most reliable tool available for selecting the

most appropriate areas in directed biopsies and exhibits a satisfactory correlation with histological analysis (Fig. 24.7). The absence of areas with increased capillary density on DSC-MRI acquisitions exhibits a reliable correlation with the absence of anaplasia, i.e., with low histological grades [36, 39].

In this regard, special attention must be paid to mixed glial tumors, which include areas comprising at least two different astrocytic, oligodendrocytic, and/or ependymal cell lineages. The differentiation between diffuse astrocytomas and WHO grade II oligodendrogliomas

is highly important given that these are well-defined clinical-pathological entities with different biological characteristics and prognoses that require different therapeutic approaches [56]. Although a focal area of oligodendrogliomas within an astrocytoma does not ensure the presence of a favorable genotype [57], molecular studies may contribute to establish prognostic criteria and better therapeutic options. Conversely, the presence of anaplastic areas within diffuse astrocytomas entails well-defined prognostic and therapeutic implications. A heterogeneous PWI map on DSC-MRI with a predominance of low rTBV values associated with elevated rTBV in a focal area is a frequent finding that must be interpreted with particular clinical attention. In such cases, the high-perfusion area (rTBV ≥ 1.75) must be the target of the directed biopsy, as it will allow for distinguishing between anaplastic areas and the oligodendroglial component and thus will enable the accurate determination of the histological diagnosis and the neoplasm grade.

Diffuse astrocytomas may occasionally exhibit high rTBV values that are directly correlated with VEGF immunorexpression [58]. According to our understanding, hyperperfusion does not exclusively reflect microvascular proliferation, which alone provides a criterion for histological grading. Given that the available system of neoplasm grading is not precise and that astrocytomas are histologically heterogeneous and may actually present a continuum of a same disease, it has been speculated that elevated rTBV might have prognostic implications. Longer follow-up periods are required (1) to validate the hypothesis that posits a correlation between the high rTBV values that are found in these cases and a higher risk of progression into higher-grade neoplasms and (2) to enable the use of such data in prognosis estimation.

Although it is possible to demonstrate overlapping findings of high rTBV with elevated metabolic relationships of spectral curves (Cho/NAA) and reduced ADC values, the spatial resolution of the DSC-MRI maps makes this method easier to use in clinical routine (e.g., for stereotactic biopsies).

24.2.4 The Assessment of the Affection of Eloquent Areas of Brain Parenchyma

Functional sequences of cortical activation are based on the physical phenomenon that is referred to as BOLD (blood-oxygen-level-dependent effect). Briefly, a specific area of the brain parenchyma is stimulated, causing a transient increase in the blood flow in that area and a consequent increase in the oxyhemoglobin supply. The diamagnetic effect of this increase transiently increases the signal of the area, thus “demarcating” the activated area. Therefore, the functional sequences that are employed to estimate cortical activation require the cooperation of patients, who are requested to perform preestablished tasks, i.e., paradigms that may consist

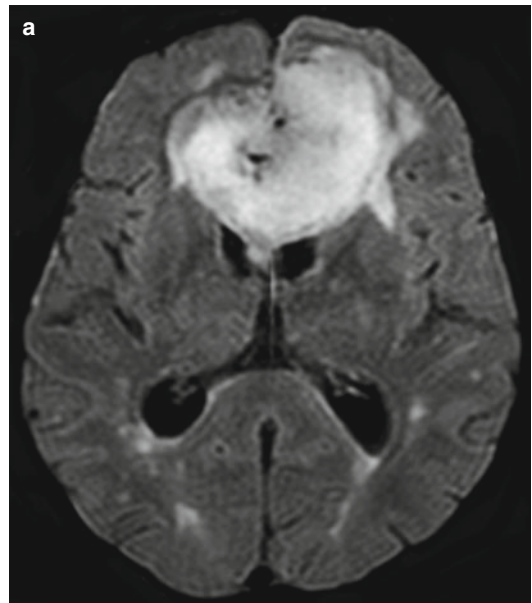


Fig. 24.6 Glioblastoma of the corpus callosum (WHO grade IV). Axial FLAIR image (a) demonstrating a “butterfly appearance” of a frontal glioblastoma crossing the midline in the genu of the corpus callosum. DSC-MRI (b) showed high capillary density with hyperperfused areas. Note the curve pattern from the tumor (green line) with a contrast leaking. MRS with short TE (31 ms) (c) showed reduced NAA peak (2.0 ppm) associated with elevated choline (3.2 ppm) and very high peaks of lipids (0.9–1.3 ppm). Color-coded image of tractography (d) demonstrated predominant destruction of the genu of the corpus callosum

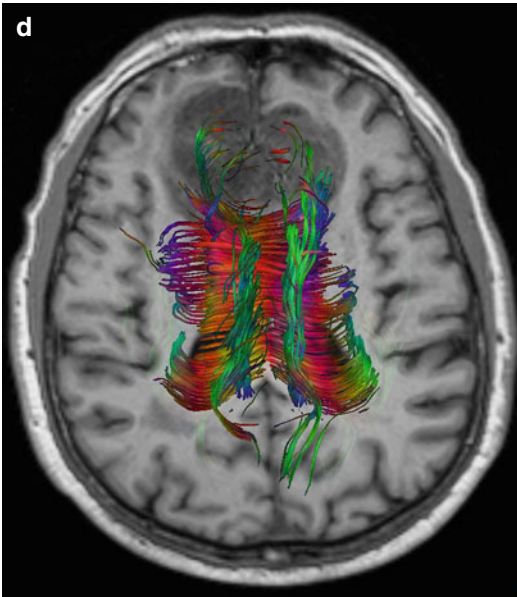


Fig. 24.6 (continued)

of a simple motor activity or involve visual or auditory stimuli, as well as language, cognitive, or tactile activities [59].

These techniques may be used to map cortical functions and eloquent areas during the surgical planning of intracranial tumors, epileptic foci, or cerebral vascular malformations. The eloquent cortex may be displaced or infiltrated by such processes, and preoperative mapping may minimize the risk of surgery, which may cause deficits in addition to those already present [59, 60]. In addition, BOLD sequences may further contribute to surgical planning by indicating the best access paths to the lesion or the requirement to perform intraoperative neurophysiological studies [60, 61]. Nevertheless, despite the increasing availability of theoretical data and clinical studies, cortical mapping is limited to a small number of centers, and its results are controversial when compared to those of intraoperative electrophysiological studies.

MR tractography may also be used to define the best surgical approach given that it shows the repercussions of the anatomical distortions on the white matter tracts; thus, this technique may prevent the surgical procedure from causing further damage. Whereas the BOLD technique is more

useful for mapping cortical areas in the case of superficial tumors, tractography has been proven to be more useful in the surgical planning of deep expansive lesions.

24.2.5 Differentiation from Other Types of Processes

MR is the standard technique that is used to identify and characterize various CNS neoplastic lesions, and its sensitivity is greater compared to other modalities that are available for both the presumptive diagnosis of neoplasms and the recognition of pseudoneoplastic conditions. Although the aim of imaging-based diagnostic techniques is not to establish the histological diagnosis of CNS neoplasms, several parameters of image interpretation are useful in the differential diagnosis of intra-axial lesions. The application of a multi-parametric approach that combines the information provided by conventional and nonconventional MR in the differentiation between the various types of neoplastic and nonneoplastic intra-axial brain lesions has previously been proven to be useful in clinical practice [62]. Despite the practical application of this combined strategy, the examiner's perspicacity is indispensable in the attribution of value to clinical-radiological details.

Several findings must be highlighted regarding the differentiation between neoplastic and nonneoplastic lesions, including the number of lesions (single versus multiple), the occurrence and pattern of Gd enhancement (nodular, ring shaped, or heterogeneous), the predominant appearance of the parenchymal lesion (infiltrative versus expansive), the occurrence of necrosis and its pattern on diffusion imaging (restriction versus facilitation), the cellularity estimates on diffusion imaging (restriction – hypercellular versus facilitation – hypervascular), as well as the findings on PWI acquisitions. Particularly among these types of images are increased capillary density (capillary neoangiogenesis on DSC-MRI) or increased permeability of the BBB on T1-weighted permeability studies (DCE-MRI). Moreover, spectral assessment may supply additional information

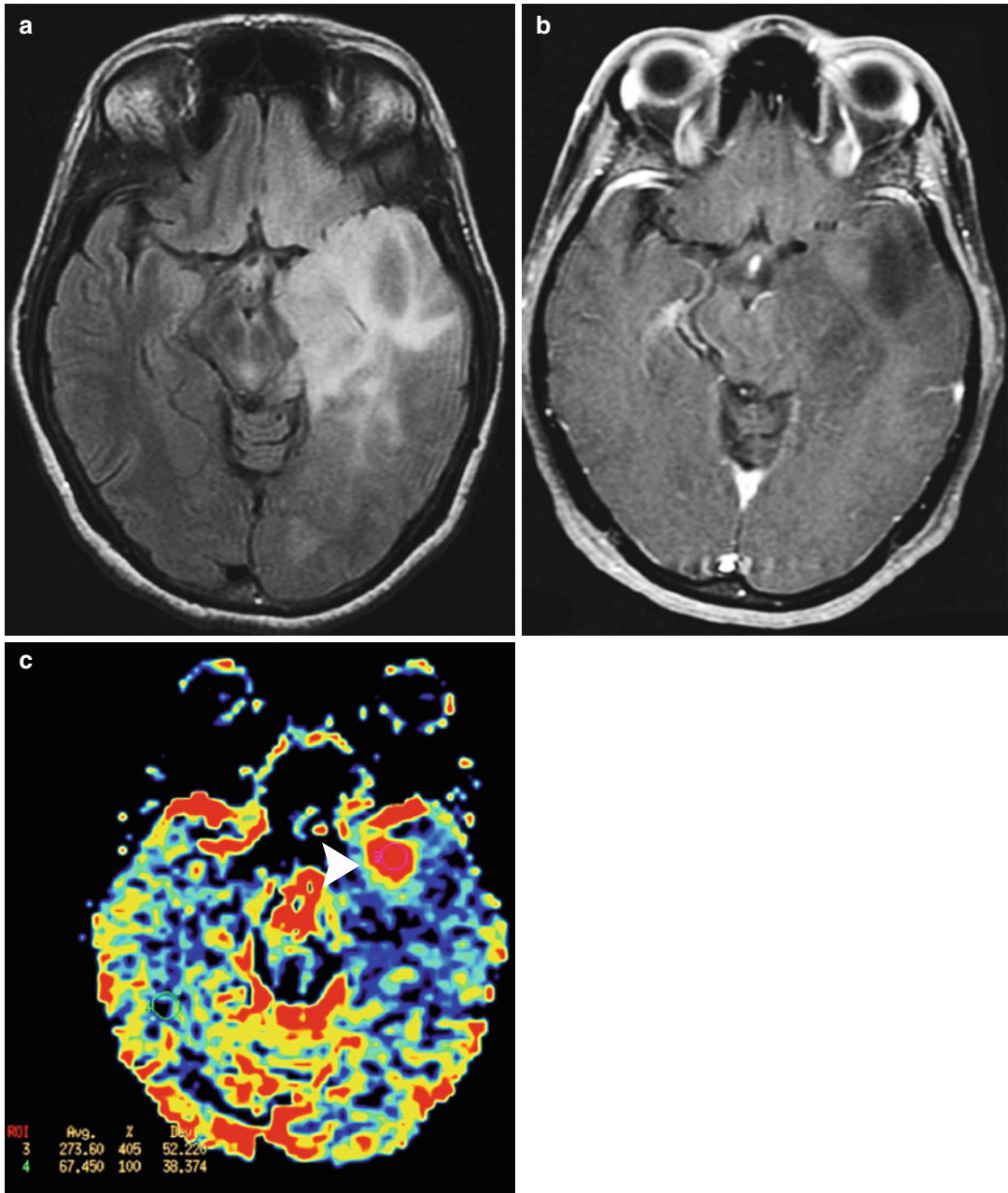


Fig. 24.7 Guiding stereotactic biopsy procedure in a diffuse glioma using DSC-MRI. A diffuse glioma was demonstrated on axial FLAIR (a) and T1WI after Gd administration (b) images. No enhancement was depicted.

DSC-MRI (c) was useful to identify an unsuspected area with hyperperfusion ($rTBV > 1.75$) (arrowhead) which was biopsied and demonstrated anaplastic features into a diffuse astrocytoma (WHO grade III)

as to the metabolic patterns of the lesions and adjacent tissue.

DWI exhibits more than 90 % sensitivity and specificity in differentiating between

epidermoid tumors (low ADC) and arachnoid cysts (high ADC), in addition to abscesses (low ADC) and necrotic tumors (high ADC). The viscosity of keratin together with the cholesterol

content of epidermoid tumors, as well as the pus viscosity together with the cell content of abscesses, result in very low ADCs, allowing for them to be distinguished from lesions with increased diffusivity in necrotic tumors or normal or slightly reduced diffusivity in demyelinating plaques [63].

Low ADC values in an intra-axial neoplasm should raise the suspicion of lymphoma or metastasis depending on the appearance of the lesion on conventional MR images, since the greater cellularity of these lesions often produces an ADC that is significantly lower than observed in diffuse gliomas [63].

In the case of solid expansive lesions, a Cho/NAA ratio >1.9 using intermediate TE (136–141 ms) was described as significant for the presumptive diagnosis of brain neoplasms and their differentiation from other causes of lesions [64]. However, the same finding may also occasionally be observed in nonneoplastic lesions. Although the cutoff values for distinguishing between neoplastic and nonneoplastic lesions are not universal, a meta-analysis of 232 studies found that a Cho/NAA ratio >2.2 is a safe value for the purpose of differential diagnosis [62]. Such wide variation in the reported cutoff ratio may be due to differences in the techniques and technical parameters applied.

24.2.5.1 Tumefactive Demyelinating Lesion (TDL)

Multiple sclerosis (MS) is an acquired chronic inflammatory disease for which multifocal damage of the white matter is currently understood to be of immune-mediated nature. MS is characterized by multifocal brain and spinal demyelination that extend over time and space with a certain degree of progressive and inexorable axonal loss. MS affects individuals of all age groups but generally predominates among young women (2.5 females to 1 male), with an incidence peak between the third and fourth decades of life. Although the prognosis of MS is variable, its progression is frequently debilitating, leading to approximately 50 % of the patients requiring walking aids within 15 years of the initial manifestation.

Acute monophasic syndromes, including Marburg's variant of MS, Baló's concentric sclerosis, and other tumefactive forms of idiopathic demyelination, may simulate primary CNS neoplasms and pose a certain degree of difficulty for clinical and paraclinical differentiation, including the imaging-based diagnostic methods. The diagnosis of the tumefactive (pseudotumoral) form of idiopathic demyelinating diseases may pose a major diagnostic challenge even for the histopathological assessment of lesions [65, 66]. A specific diagnosis is nonetheless indispensable as a function of the therapeutic and prognostic implications, whereas biopsies must be avoided as much as possible.

MRS sequences are not particularly useful in performing this differentiation due to the overlap between the findings for TDLs and primary CNS lesions, namely, increased choline levels and ratios, reductions in the NAA peak, and the occasional presence of lipids [67, 68]. Such overlap may lead to incorrect interpretations of the results of the imaging studies and consequent unnecessary intervention treatment. Nevertheless, in the case of MS-associated TDLs, the multifocal affection may be observed in lesions other than the alteration of "normal-appearing white matter," extending beyond the limits of the tumefactive lesion, by the reduction in the NAA peak and its ratios, or even earlier by the elevation of the myoinositol peak.

TDLs exhibit variable values on ADC maps; the ADCs are primarily elevated due to increased water content of the lesions, thus contributing to the differentiation between pseudotumoral lesions and brain abscess. However, ADC maps may also exhibit decreased values, possibly due to intramyelinic edema and acute demyelinating activity. As a general rule, the pattern of Gd enhancement and the occurrence of areas with more marked reduction in ADC values coincide with the external rings of the lesions, which represent the areas of active demyelination [69].

Brain assessment by means of PWI (DSC-MRI) shows hypoperfusion inside of the lesions, whereas the rCBV is lower compared to the contralateral, normal-appearing white matter and substantially lower compared to primary

neoplasms, especially for high-grade and secondary lesions [70].

Despite the wide clinical pleomorphism and the various imaging patterns that are exhibited by idiopathic TLDs, one may assume that the conjunction of the data provided by clinical-radiological assessment, including nonconventional MR imaging acquisition, allows for a reliable diagnosis in the majority of cases. It is suggested that special value be attributed to the presence of lesions with “open-ring” enhancement, a peripheral restriction on DWI, the occurrence of venous ectasia inside or in the periphery of lesions, and the characterization of glutamine/glutamate levels (Glx, 2.4 ppm) in the recognition of tumefactive demyelination and its appropriate differentiation from neoplasms (Fig. 24.8) [71].

24.2.5.2 Pyogenic Brain Abscess

Brain abscesses are infrequent but severe complications of infectious processes, generally bacterial, that are due to the hematogenous dissemination of an extracranial infectious focus, the extension of meningeal or nasal sinus infections, trauma, or postoperative conditions. Moreover, pulmonary arteriovenous fistulas represent a risk factor for the development of a brain abscess.

The clinical manifestations are uncharacteristic, determined by the mass effect without other signs indicative of infection, such as fever and signs of meningeal irritation. Under such conditions, differential diagnosis with expansive lesions, high-grade tumors in particular, or even single metastatic lesions may pose a challenge when it is exclusively based on the findings from conventional sequences. Abscesses are generally diagnosed in their capsular stage as lesions with necrotic/liquefied centers, the contents of which exhibit increased signal on T2/FLAIR-weighted sequences, and peripheral Gd enhancement (ring-shaped pattern). The capsule is generally smooth, fine, and regular; it may be finer when it is more proximal to the ventricle and seldom exhibits irregular contours when the etiological agent is a pyogenic bacteria.

MRS sequences may be useful for differential diagnosis as its metabolic characteristics

are unusual in other pathological processes, particularly the presence of amino acids, such as valine, leucine, and isoleucine. These amino acids are the final product of the proteolytic action of enzymes released by neutrophils within the area of liquefactive necrosis that occurs in pyogenic abscesses. Abscesses may also contain other metabolites, such as lactate, acetate, succinate, and alanine, which accumulate from the tissue necrosis and from several fermentative and glycolytic pathways. The presence of acetate and succinate has been attributed to infections by anaerobic bacteria [72, 73].

Diffusion-weighted imaging (DWI) lends greater specificity to diagnosis as it shows the restriction to the free motion of the water molecules as estimated by the ADC map values inside of the abscess' purulent content. Additionally, DWI is the functional sequence with the greatest sensitivity and reveals ADC reduction even in the earliest stages of cerebritis and small-sized lesions [74]. However, attention must be paid to potentially mimetic factors, including a heterogeneous hypersignal on diffusion-weighted sequences, which is observed for tumor lesions with necrotic content and subacute hemorrhages (metahemoglobin). The presence of products of hemoglobin degradation alters the homogeneity of the local magnetic field and restricts the diffusivity of the water molecules. The correlation with other findings on conventional imaging, in particular the sequences with greatest magnetic susceptibility (T2* or SWI), as well as functional sequences, such as PWI and MRS, contributes to the differential diagnosis.

Recently, the application of SWI to the differentiation between abscess and necrotic glioblastoma was emphasized through the analysis of the MR signal of the lesion capsule [75]. Although both lesions exhibit a hypointense rim on T2, SWI confirms the presence of regular and complete contours in abscesses, in which the hypointense rim further coincides with the localization of Gd enhancement (post-Gd T1W1). In addition, only abscesses exhibit the “dual rim sign,” which is defined by the presence of two concentric rings, of which the most external is hypointense (Fig. 24.9).

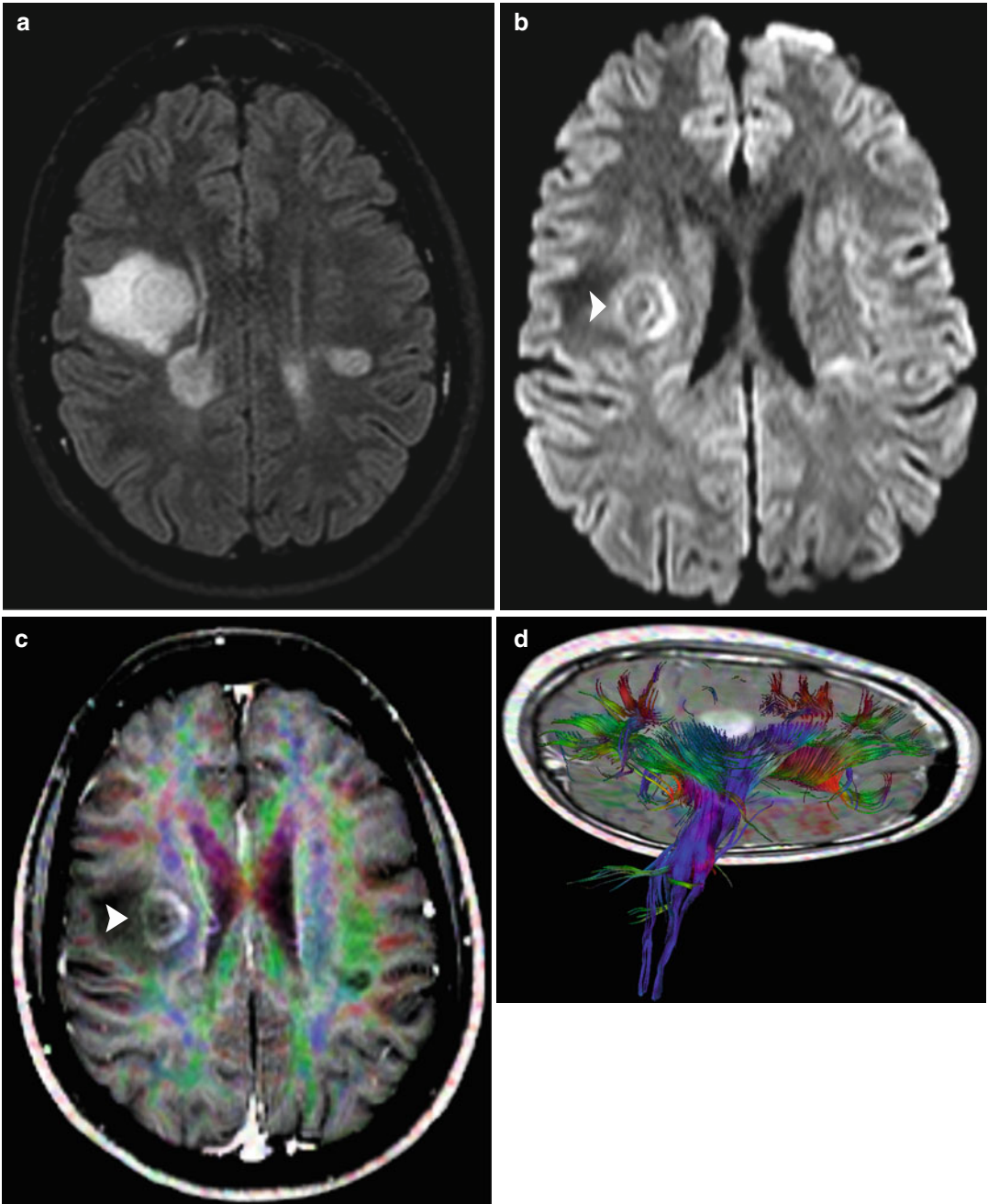


Fig. 24.8 Tumefactive demyelinating lesion. Axial FLAIR image (**a**) showed an atypical lesion associated with vasogenic edema (pseudotumoral demyelination) in the right centrum semiovale. The diagnosis of multiple sclerosis was defined on clinical and paraclinical features. Axial DWI (**b**) showed concentric zones of restricted water diffusion (*arrow head*) that correlates to active demyelination characterized by an “open-ring

enhancement” after Gd administration. Axial T1WI after Gd administration was superimposed to directional map of DTI (**c**) to demonstrate predominant medial displacement of right corticospinal tract (*arrow head*). It was confirmed on tractography (**d**). MRS with short TE (31 ms) showed preserved NAA peak with moderate elevation in choline/creatine ratio and high Glx and lactate peaks (**e**)

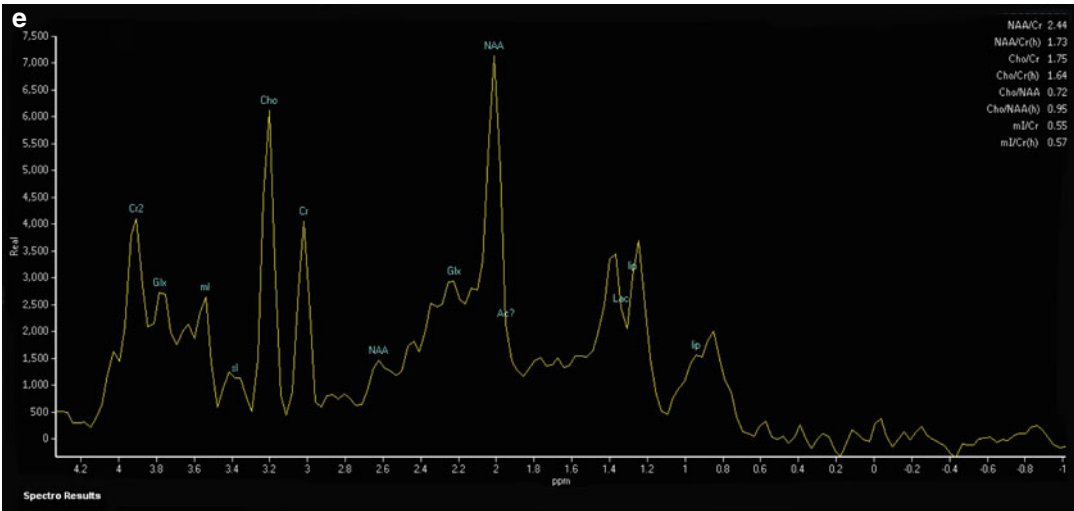


Fig. 24.8 (continued)

In pyogenic abscesses, DSC-MRI shows low rCBV values, contrary to the expected values for high-grade tumors. Occasionally, with the chronicity of the inflammatory process, rCBV levels may increase in the capsule of late abscesses, which may hinder the differential diagnosis.

Brain abscesses may be caused by various etiological agents, including fungi, protozoa, and mycobacteria, and others. Certain particularities have previously been noted on conventional and nonconventional MR that allow for inferring the exact etiology [76]. Fungal abscesses occur more often among immunosuppressed or neutropenic individuals and generally exhibit irregular, ring-shaped Gd enhancement. Angioinvasive agents, such as *Aspergillus* and mucormycosis, may be associated with hemorrhage. Tuberculosis poses a diagnostic problem in several parts of the world, particularly among immunocompromised individuals, given that its progression is subacute and afebrile. The MR patterns differ for this condition from those of the pyogenic abscesses by simulating primary or secondary brain neoplasms [77]. Within an appropriate context, the presence of a lipid peak in the absence of amino acids increases the odds of a lesion being a tuberculosis abscess [77].

24.3 The Use of PET in the Assessment of Gliomas

Structural MR imaging studies provide information regarding the size and location of tumors and their secondary effects, such as mass effect, edema, hemorrhage, necrosis, and signs of intracranial hypertension. In comparison, positron emission tomography (PET) allows for the noninvasive assessment of metabolic and molecular features that may lead to the development of customized treatment regimens and facilitate the assessment of pre- and posttreatment prognosis.

Depending on the radiotracer that is used, different molecular processes may be analyzed, although most such agents are related to intratumoral cell proliferation [78]. Several radiotracers were suggested to accomplish different goals in the assessment of gliomas, such as diagnosis, histological grading, surgical planning, the assessment of relapses, and the monitoring of treatment. The most important and promising approaches include the following:

Glucose metabolism – The glucose analog 2-[¹⁸F] fluoro-2-deoxy-D-glucose ([¹⁸F]FDG) is the most widely used radiotracer to measure the local glucose consumption, which represents the common pathway of the brain neurochemical